Lectures on the Cosmic Microwave Background

Raphael M. Flauger
The University of Texas

Summer School on Cosmology, ICTP, June 2016

Lecture IV

- Measurement of angular power spectrum and parameter constraints (continued)
- More on primordial anisotropies
- Search for primordial gravitational waves
- Outlook

Planck Angular Power Spectrum

- Launched on May 14, 2009
- Observed "from" L2 from August 12, 2009
- End of observations for HFI January 2012
- End of observations for LFI August 2013
- Temperature data for "nominal" mission released on March 21, 2013

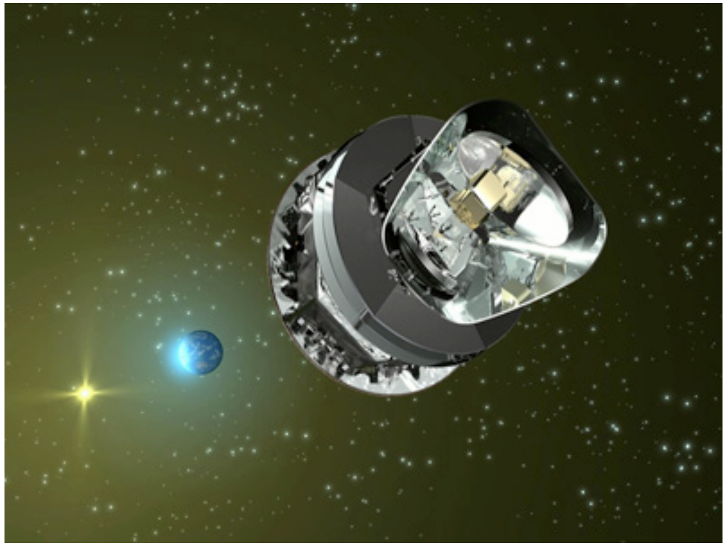

- First release of full mission data on February 5, 2015

Planck Angular Power Spectrum

The likelihood is a hybrid of a

- pixel space likelihood for low ℓ
  (T mostly constrains amplitude, P mostly constrains optical depth)
- fiducial Gaussian approximation for high ℓ

	2013	2015
low-ℓ T	Commander ($f_{\rm sky} = 0.87$)	Commander ($f_{\rm sky} = 0.93$)
low-ℓ P	WMAP($f_{\rm sky} = 0.76$)	Planck LFI($f_{\rm sky} = 0.47$)
high-ℓ	CAMspec	Plik

Planck Angular Power Spectrum

The high-ℓ likelihoods for are based on

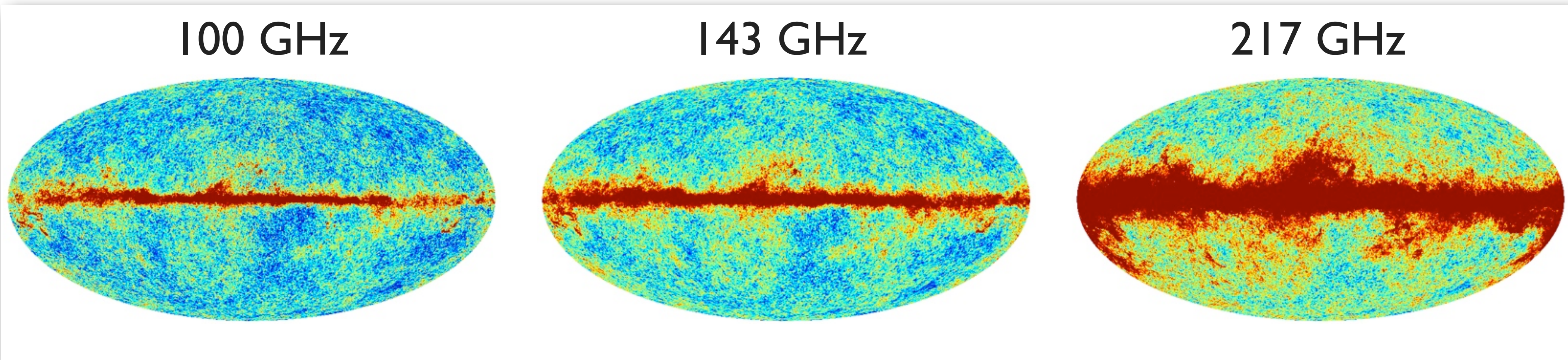

- 100x100 spectra up to $\ell = 1200$
- 143x143 spectra up up to $\ell = 2000$
- 143x217 and 217x217 spectra up to $\ell = 2500$

Planck Angular Power Spectrum

- masks for galactic and point source emission

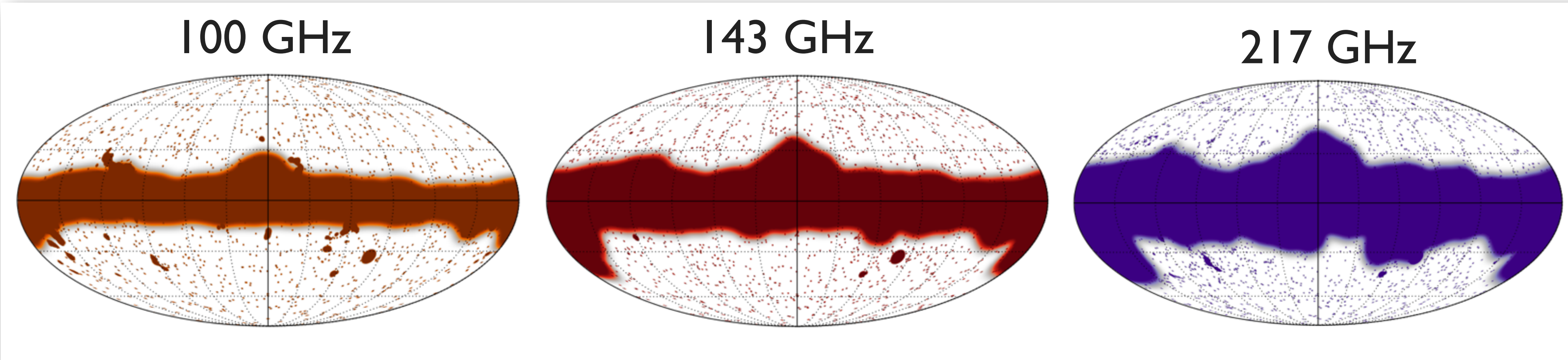

- power spectrum templates to model diffuse galactic emission and extragalactic foregrounds
- analytic, fiducial Gaussian approximation for likelihood as discussed earlier
- noise properties from fit of Planck noise model to map half-differences

Planck Angular Power Spectrum

Noise from half-mission differences

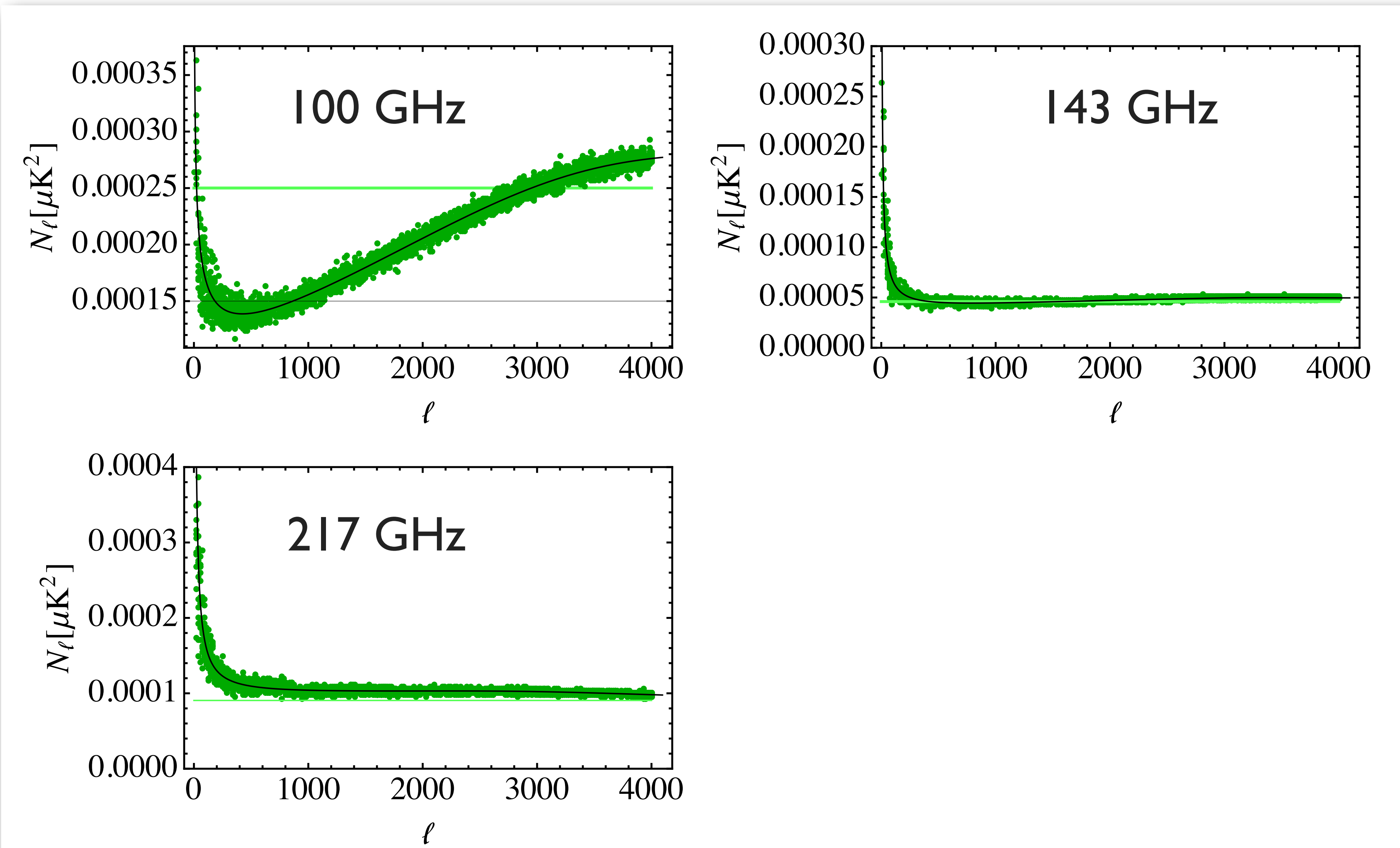

LCDM

Once we have produced a likelihood, we can run our favorite Markov Chain Monte Carlo routine

Parameter	*Planck* TT+lowP
$\Omega_b h^2$	0.02222 ± 0.00023
$\Omega_c h^2$	0.1197 ± 0.0022
$100\theta_{MC}$	1.04085 ± 0.00047
τ	0.078 ± 0.019
$\ln(10^{10} A_s)$	3.089 ± 0.036
n_s	0.9655 ± 0.0062
H_0	67.31 ± 0.96
Ω_m	0.315 ± 0.013
σ_8	0.829 ± 0.014
$10^9 A_s e^{-2\tau}$	1.880 ± 0.014

LCDM+X

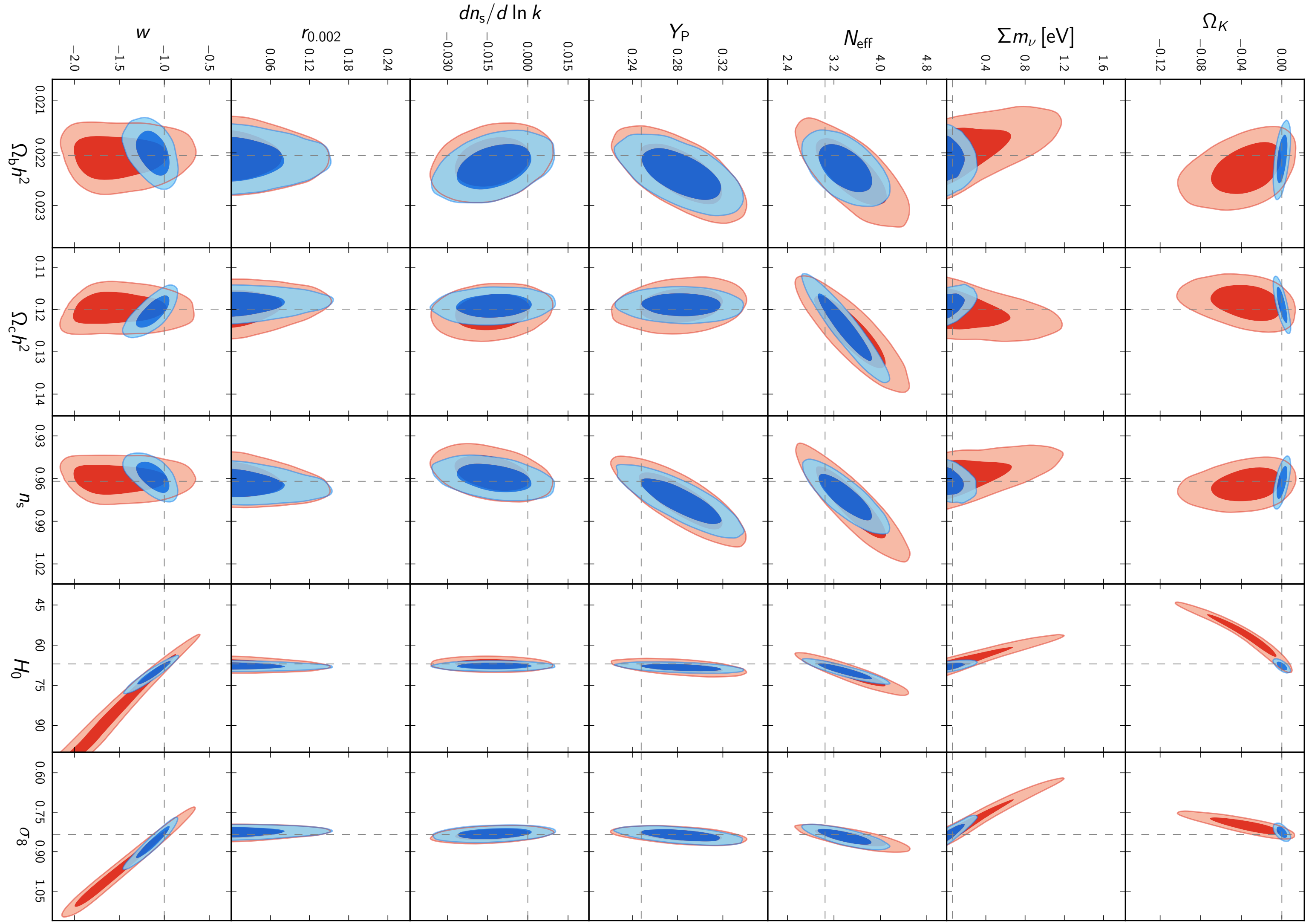

Planck+WP

Planck+WP+BAO

More on temperature anisotropies

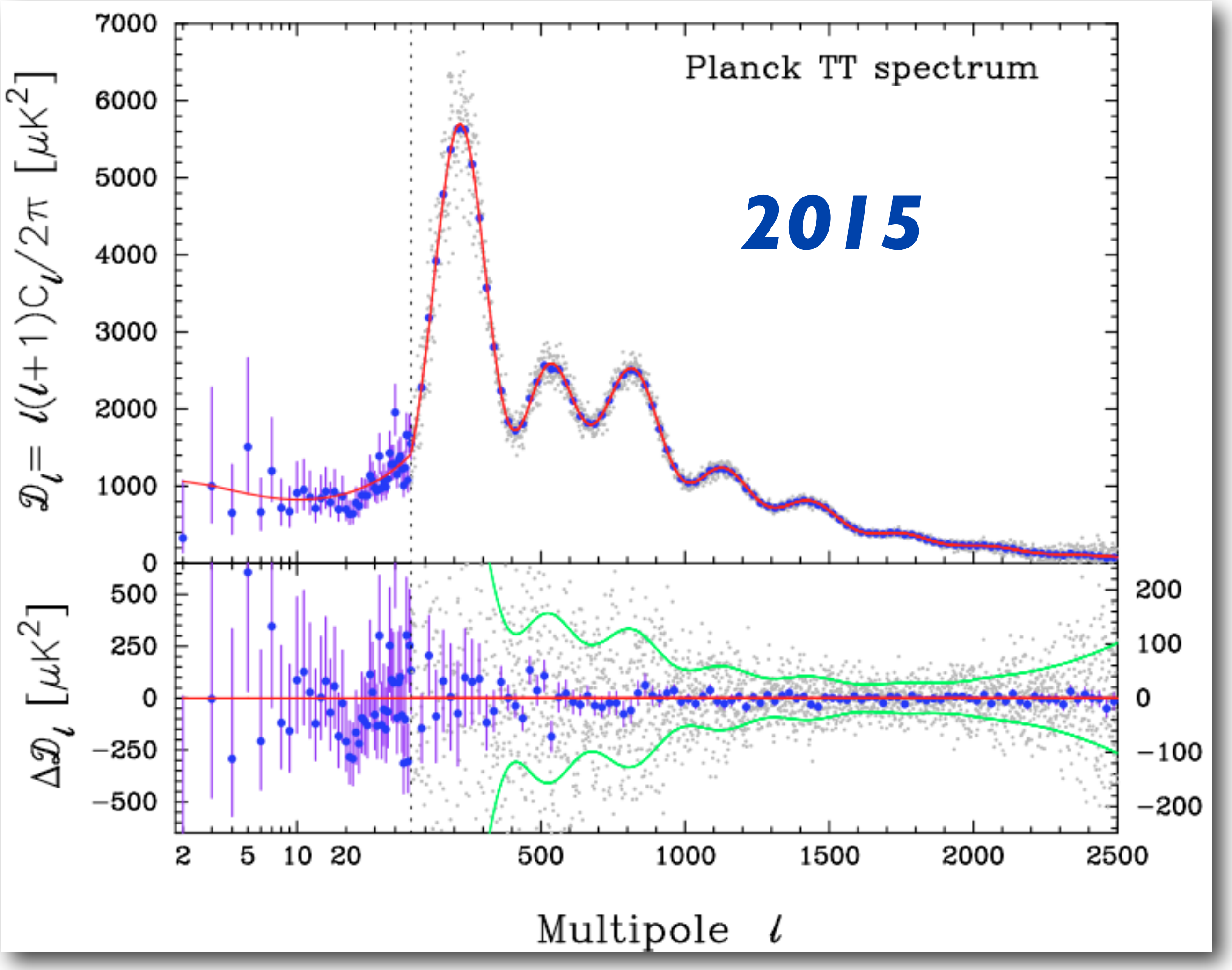

More on temperature anisotropies

Recall that the temperature anisotropy is given by

$$\frac{\Delta T(\hat{n})}{T_0} = \frac{1}{4}\Delta_T(\vec{x}=0,-\hat{n},t_0)$$

where $\Delta_T(\vec{x},\hat{p},t_0)$ satisfies a Boltzmann equation.

We looked for solutions of the form

$$\Delta_T(\vec{x},\hat{p},t) = \int \frac{d^3q}{(2\pi)^3}\alpha(\vec{q})\Delta_T(q,\mu,t)e^{i\vec{q}\cdot\vec{x}}$$

and expanded $\Delta_T(q,\mu,t)$ in terms of Legendre polynomials

$$\Delta_T(q,\mu,t) = \sum_\ell (-i)^\ell(2\ell+1)P_\ell(\mu)\Delta_{T,\ell}(q,t)$$

to arrive at the Boltzmann hierarchy.

More on temperature anisotropies

For scalar perturbations

$$\dot{\Delta}^{(S)}_{T,\ell}(q,t) + \frac{q}{a(2\ell+1)}\left[(\ell+1)\Delta^{(S)}_{T,\ell+1}(q,t) - \ell\Delta^{(S)}_{T,\ell-1}(q,t)\right]$$
$$= -\omega_c(t)\Delta^{(S)}_{T,\ell}(q,t) - 2\dot{A}_q\delta_{\ell,0} + 2q^2\dot{B}_q\left(\frac{1}{3}\delta_{\ell,0} - \frac{2}{15}\delta_{\ell,2}\right)$$
$$+\omega_c\Delta^{(S)}_{T,0}\delta_{\ell,0} + \frac{1}{10}\omega_c\Pi\delta_{\ell,2} - \frac{4}{3}\frac{q}{a}\omega_c\delta u_{b\,q}\delta_{\ell,1}$$

$$\dot{\Delta}^{(S)}_{P,\ell}(q,t) + \frac{q}{a(2\ell+1)}\left[(\ell+1)\Delta^{(S)}_{P,\ell+1}(q,t) - \ell\Delta^{(S)}_{P,\ell-1}(q,t)\right]$$
$$= -\omega_c(t)\Delta^{(S)}_{P,\ell}(q,t) + \frac{1}{2}\omega_c(t)\Pi(q,t)\left(\delta_{\ell,0} + \frac{1}{5}\delta_{\ell,2}\right)$$

Let’s undo the last step and consider the equation satisfied by $\Delta^{(S)}_{T}(q,\mu,t)$.

More on temperature anisotropies

$$\dot{\Delta}_T^{(S)}(q,\mu,t) + i\frac{q\mu}{a(t)}\Delta_T^{(S)}(q,\mu,t) = -\omega_c(t)\Delta_T^{(S)}(q,\mu,t)$$
$$+\omega_c\Delta_{T,0}^{(S)}(q,t) - \frac{1}{2}\omega_c P_2(\mu)\Pi(q,t)$$
$$+\frac{4iq\mu}{a(t)}\omega_c(t)\delta u_{B\,q}(t) - 2\dot{A}_q(t) + 2q^2\mu^2\dot{B}_q(t)$$

$$\dot{\Delta}_P^{(S)}(q,\mu,t) + i\frac{q\mu}{a(t)}\Delta_P^{(S)}(q,\mu,t) = -\omega_c(t)\Delta_P^{(S)}(q,\mu,t)$$
$$+\frac{3}{4}\omega_c(t)(1-\mu^2)\Pi(q,t)$$

with source function

$$\Pi \quad = \quad \Delta_{P,0}^{(S)} + \Delta_{T,2}^{(S)} + \Delta_{P,2}^{(S)}$$

More on temperature anisotropies

The formal solution obtained by line-of-sight integration

$$\Delta_T^{(S)}(q,\mu,t_0) = \int_{t_1}^{t_0} dt\ \exp\left[-iq\mu\int_t^{t_0}\frac{dt'}{a(t')} - \int_t^{t_0} dt'\omega_c(t')\right]$$

$$\times\left\{\omega_c\left[\Delta_{T,0}^{(S)} - \frac{1}{2}P_2(\mu)\Pi(q,t) - 2a^2(t)\ddot{B}_q(t) - 2a(t)\dot{a}(t)\dot{B}_q(t)\right.\right.$$

$$\left. + 4i\mu q\left(\delta u_q(t)/a(t) + a(t)\dot{B}_q(t)/2\right)\right]$$

$$\left. - \frac{d}{dt}\left(2A_q(t) + 2a^2(t)\ddot{B}_q(t) + 2a(t)\dot{a}(t)\dot{B}_q(t)\right)\right\}$$

shows that the temperature perturbations consist of two contributions

$$\left(\frac{\Delta T(\hat{n})}{T_0}\right)^{(S)} = \left(\frac{\Delta T(\hat{n})}{T_0}\right)^{(S)}_{LSS} + \left(\frac{\Delta T(\hat{n})}{T_0}\right)^{(S)}_{ISW}$$

More on temperature anisotropies

$$\left(\frac{\Delta T(\hat{n})}{T_0}\right)^{(S)}_{LSS} = \int \frac{d^3q}{(2\pi)^3}\alpha(\vec{q})$$

$$\times \int_{t_1}^{t_0} dt\ \exp\left[-iq\mu\int_t^{t_0}\frac{dt'}{a(t')}\right]\exp\left[-\int_t^{t_0} dt'\omega_c(t')\right]\omega_c(t)$$

$$\times\left[\frac{1}{4}\Delta^{(S)}_{T,0}(q,t) - \frac{1}{8}P_2(\mu)\Pi(q,t) - \frac{1}{2}a^2(t)\ddot{B}_q(t) - \frac{1}{2}a(t)\dot{a}(t)\dot{B}_q(t)\right.$$

$$\left. + i\mu q\left(\delta u_q(t)/a(t) + a(t)\dot{B}_q(t)/2\right)\right]$$

More on temperature anisotropies

$$\left(\frac{\Delta T(\hat{n})}{T_0}\right)^{(S)}_{LSS} = \int \frac{d^3q}{(2\pi)^3}\alpha(\vec{q})$$

Last scattering probability

$$\times \int_{t_1}^{t_0} dt \;\exp\left[-iq\mu\int_t^{t_0}\frac{dt'}{a(t')}\right]\exp\left[-\int_t^{t_0} dt'\omega_c(t')\right]\omega_c(t)$$

$$\times\left[\frac{1}{4}\Delta^{(S)}_{T,0}(q,t) - \frac{1}{8}P_2(\mu)\Pi(q,t) - \frac{1}{2}a^2(t)\ddot{B}_q(t) - \frac{1}{2}a(t)\dot{a}(t)\dot{B}_q(t)\right.$$

$$\left. + i\mu q\left(\delta u_q(t)/a(t) + a(t)\dot{B}_q(t)/2\right)\right]$$

More on temperature anisotropies

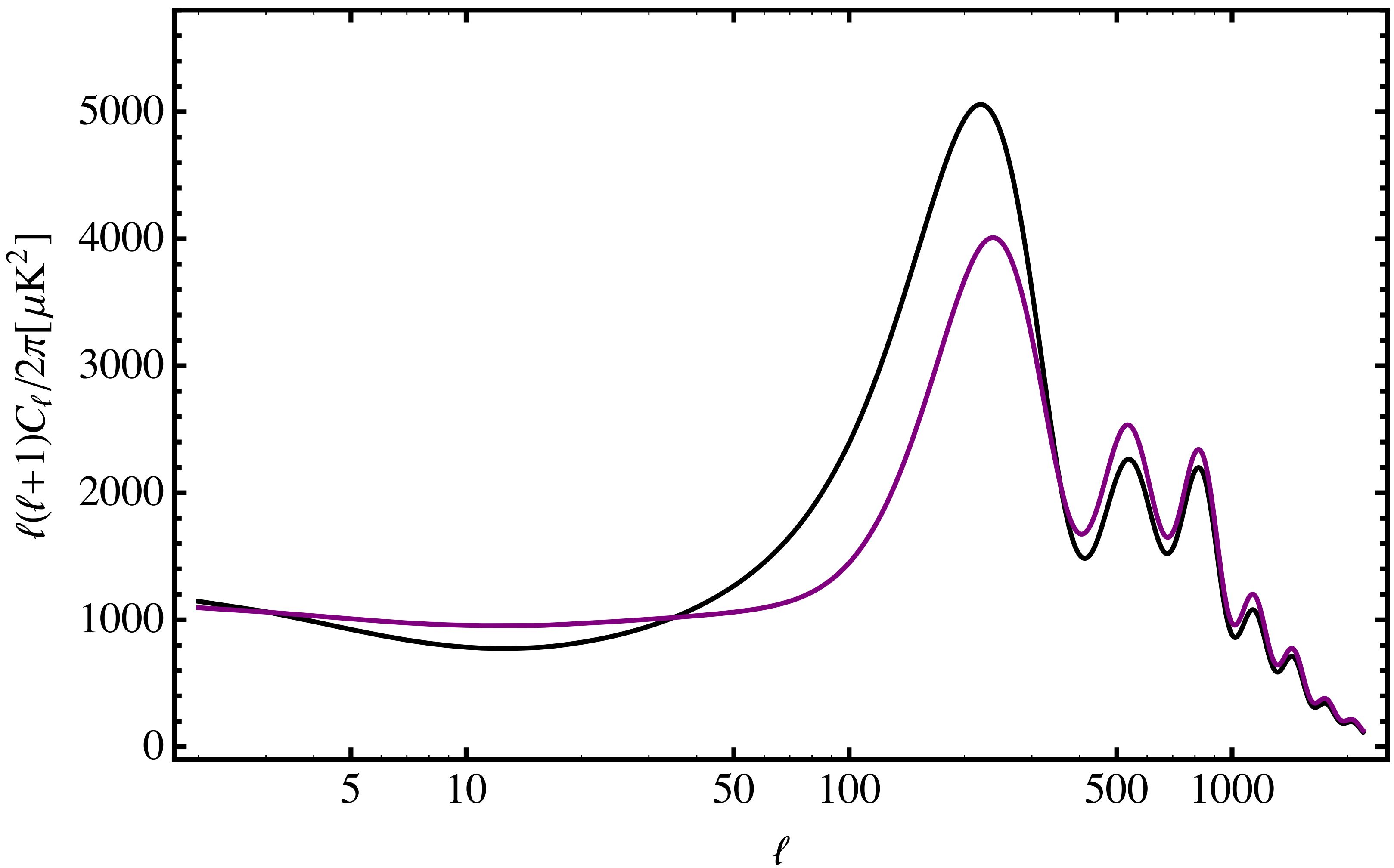

More on temperature anisotropies

$$\left(\frac{\Delta T(\hat{n})}{T_0}\right)^{(S)}_{LSS} = \int \frac{d^3q}{(2\pi)^3}\alpha(\vec{q})$$

$$\times \int_{t_1}^{t_0} dt \ \exp\left[-iq\mu \int_t^{t_0} \frac{dt'}{a(t')}\right] \exp\left[-\int_t^{t_0} dt'\omega_c(t')\right]\omega_c(t)$$

$$\times \left[\frac{1}{4}\Delta^{(S)}_{T,0}(q,t) - \frac{1}{8}P_2(\mu)\Pi(q,t) - \frac{1}{2}a^2(t)\ddot{B}_q(t) - \frac{1}{2}a(t)\dot{a}(t)\dot{B}_q(t)\right.$$

$$\left. + i\mu q\left(\delta u_q(t)/a(t) + a(t)\dot{B}_q(t)/2\right)\right]$$

Intrinsic density fluctuation and gravitational redshifting

More on temperature anisotropies

$$\left(\frac{\Delta T(\hat{n})}{T_0}\right)^{(S)}_{LSS} = \int \frac{d^3q}{(2\pi)^3}\alpha(\vec{q})$$

$$\times \int_{t_1}^{t_0} dt\ \exp\left[-iq\mu\int_t^{t_0}\frac{dt'}{a(t')}\right]\exp\left[-\int_t^{t_0} dt'\omega_c(t')\right]\omega_c(t)$$

$$\times\left[\frac{1}{4}\Delta^{(S)}_{T,0}(q,t) - \frac{1}{8}P_2(\mu)\Pi(q,t) - \frac{1}{2}a^2(t)\ddot{B}_q(t) - \frac{1}{2}a(t)\dot{a}(t)\dot{B}_q(t)\right.$$

$$\left.+i\mu q\left(\delta u_q(t)/a(t) + a(t)\dot{B}_q(t)/2\right)\right]$$

Intrinsic density fluctuation and gravitational redshifting

Doppler effect

More on temperature anisotropies

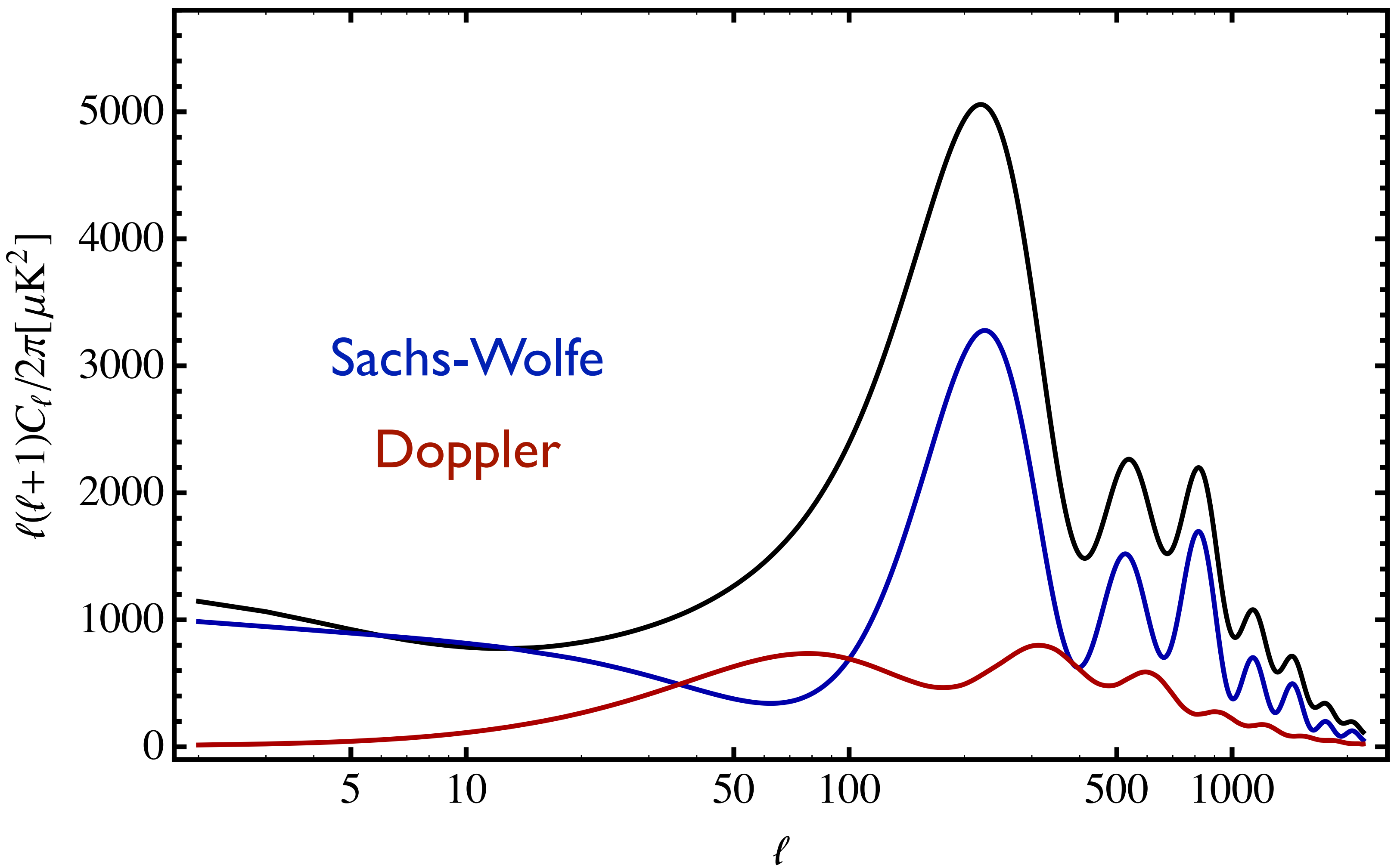

More on temperature anisotropies

Integrated Sachs-Wolfe effect

$$\left(\frac{\Delta T(\hat{n})}{T_0}\right)^{(S)}_{ISW} = -\frac{1}{2}\int \frac{d^3q}{(2\pi)^3}\alpha(\vec{q})$$

$$\times \int_{t_1}^{t_0} dt\ \exp\left[-iq\mu\int_t^{t_0}\frac{dt'}{a(t')}\right]\exp\left[-\int_t^{t_0} dt'\omega_c(t')\right]$$

$$\times \frac{d}{dt}\Big(A_q(t) + a^2(t)\ddot{B}_q(t) + a(t)\dot{a}(t)\dot{B}_q(t)\Big)$$

This contribution can be generated even in the absence of free electrons.

More on temperature anisotropies

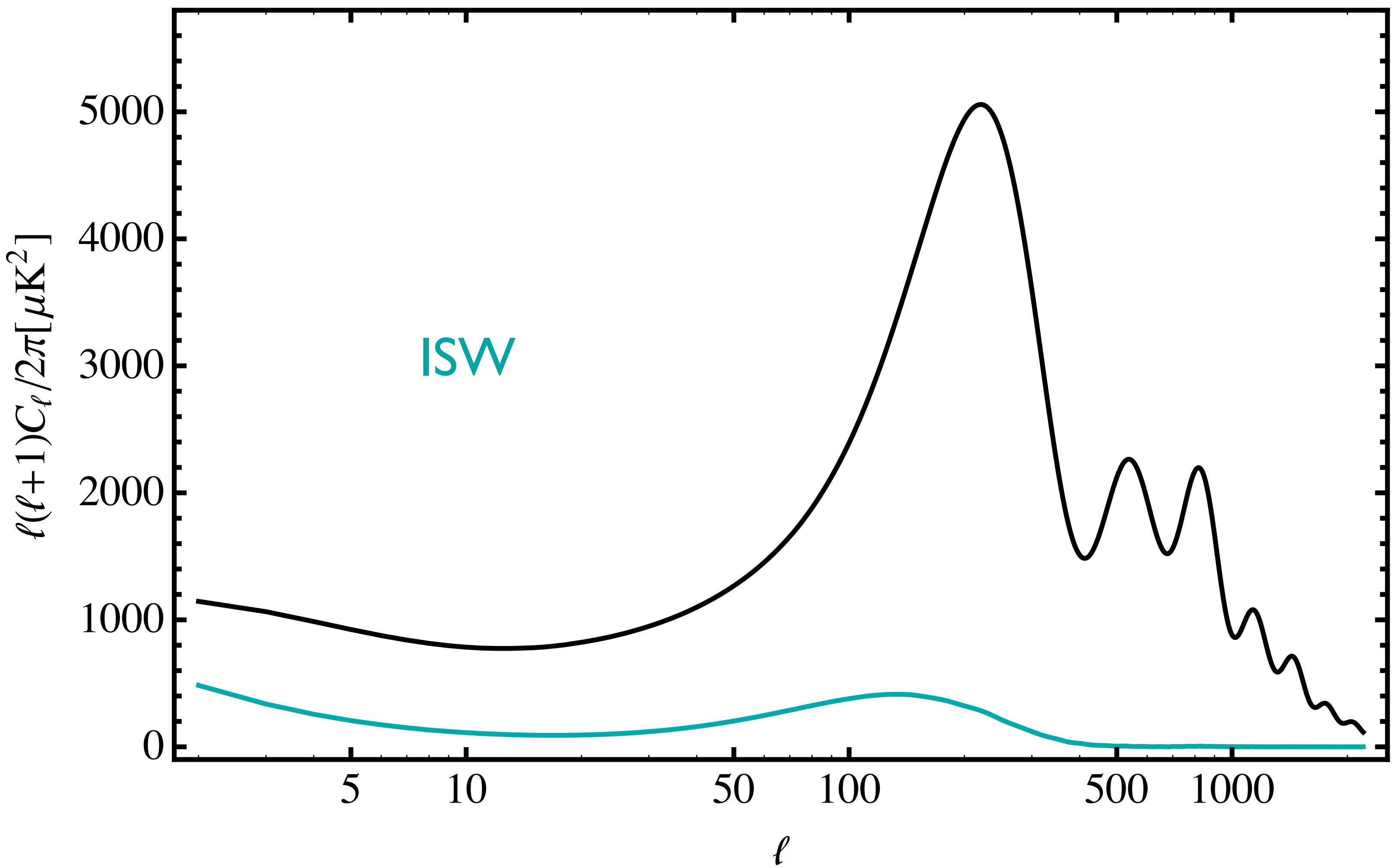

More on temperature anisotropies

During matter domination the gravitational potential does not evolve

$$\frac{d}{dt}\Big(A_q(t) + a^2(t)\ddot{B}_q(t) + a(t)\dot{a}(t)\dot{B}_q(t)\Big) = 0$$

The integrated Sachs-Wolfe effect has two contributions

early contribution:

During recombination radiation is not yet completely negligible.

late contribution:

At late times dark energy becomes important

More on temperature anisotropies

Early vs late ISW

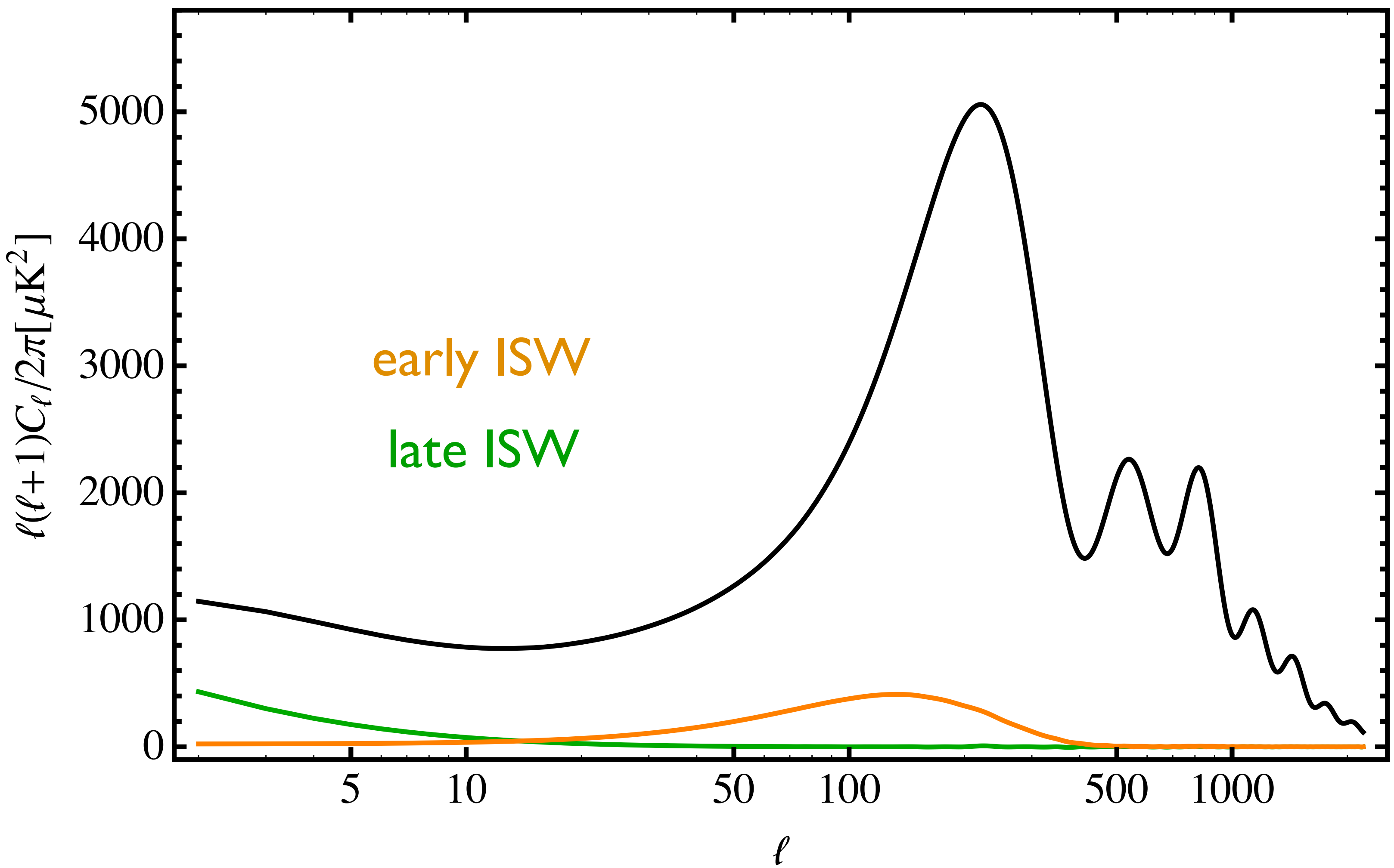

More on temperature anisotropies

Recombination vs late time contributions

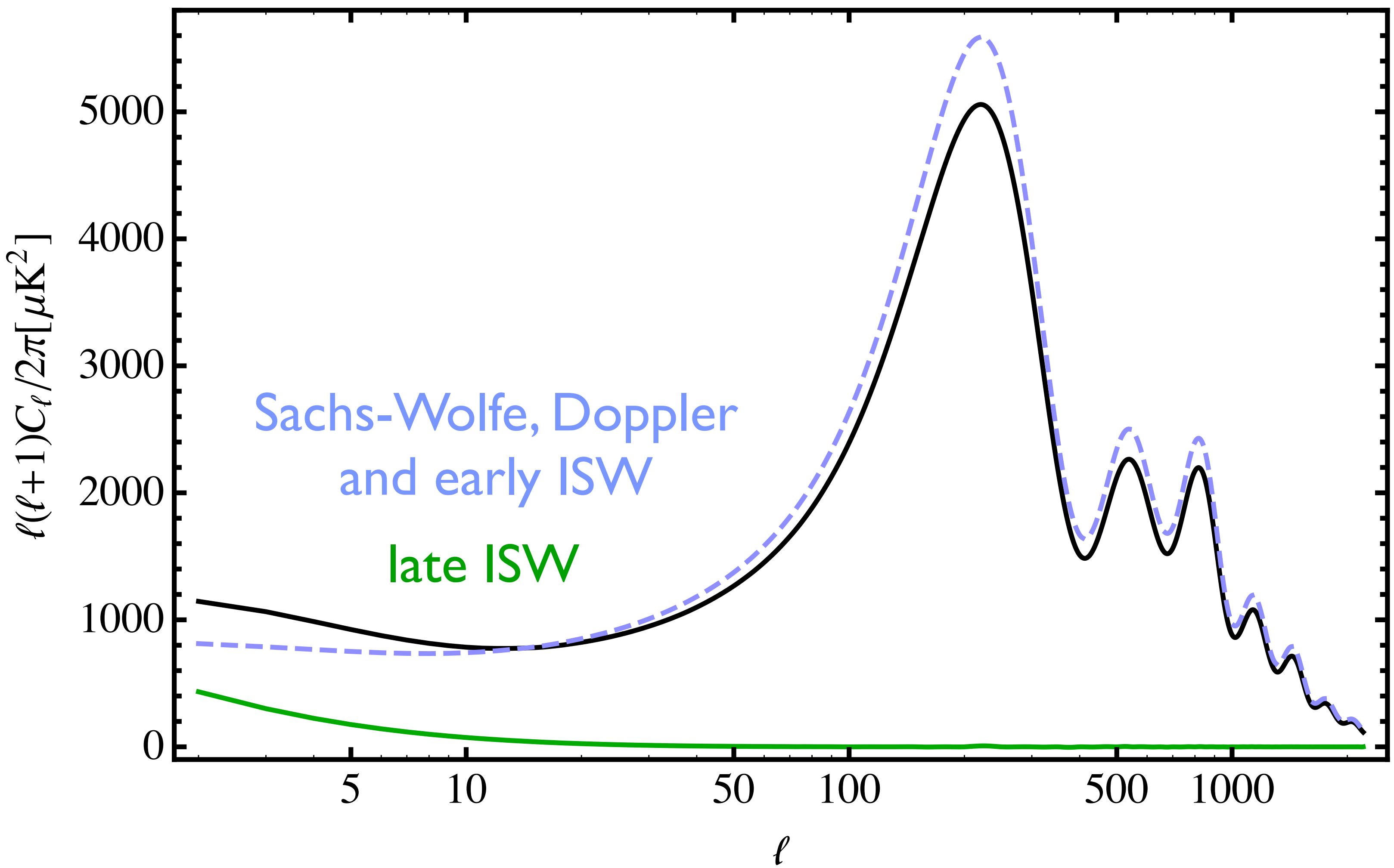

More on temperature anisotropies

Recombination vs late time contributions

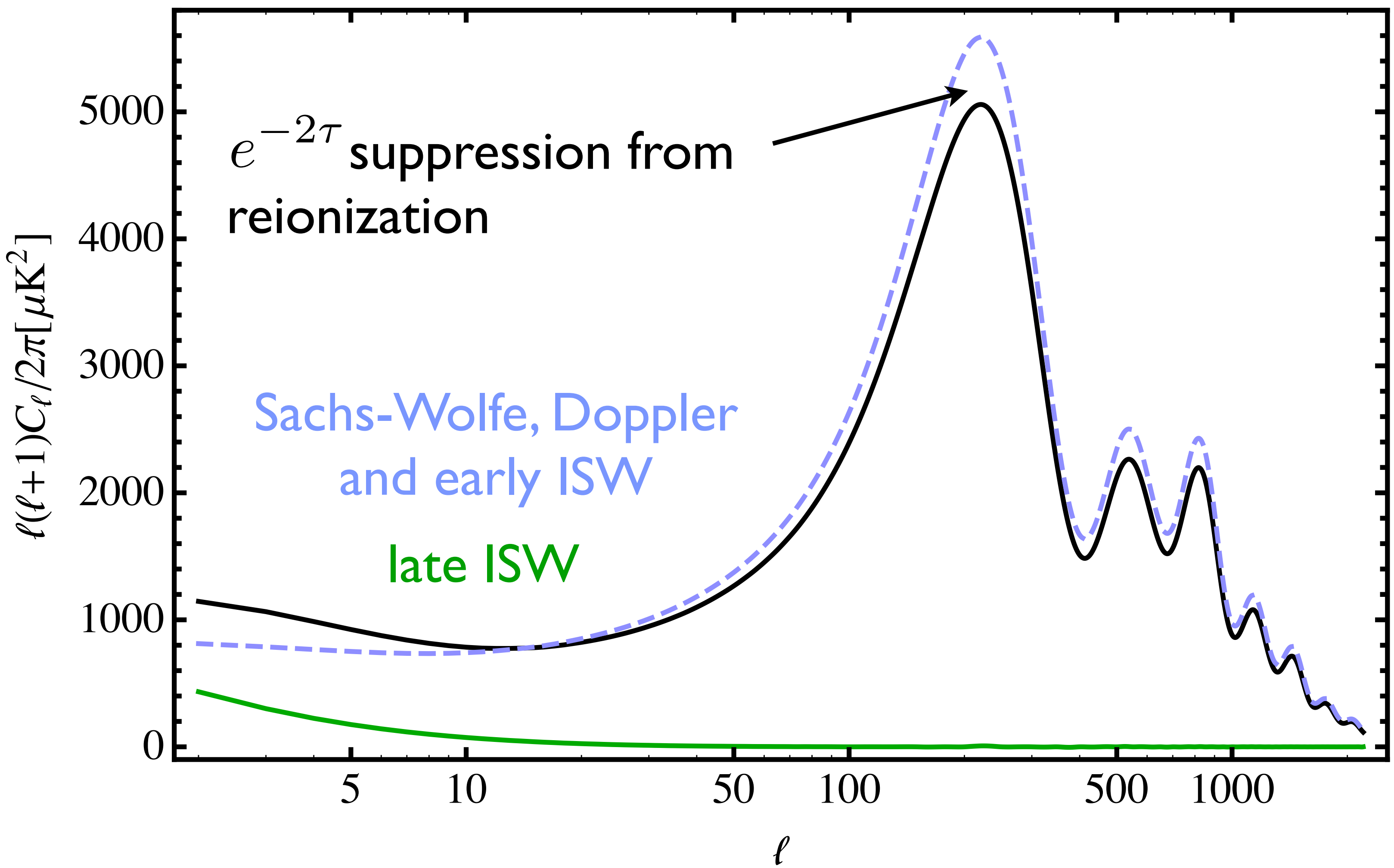

More on temperature anisotropies

Much of this can be understood analytically. Let us focus on the dominant Sachs-Wolfe and Doppler contributions

$$\left(\frac{\Delta T(\hat{n})}{T_0}\right)^{(S)}_{LSS} = \int \frac{d^3q}{(2\pi)^3}\alpha(\vec{q})$$

$$\times \int_{t_1}^{t_0} dt\ \exp\left[-iq\mu\int_t^{t_0}\frac{dt'}{a(t')}\right]\exp\left[-\int_t^{t_0} dt'\omega_c(t')\right]\omega_c(t)$$

$$\times\left[\frac{1}{4}\Delta^{(S)}_{T,0}(q,t) - \frac{1}{8}P_2(\mu)\Pi(q,t) - \frac{1}{2}a^2(t)\ddot{B}_q(t) - \frac{1}{2}a(t)\dot{a}(t)\dot{B}_q(t)\right.$$

$$\left. + i\mu q\left(\delta u_q(t)/a(t) + a(t)\dot{B}_q(t)/2\right)\right]$$

and as a first approximation set $P(t)\approx\delta(t-t_L)$.

More on temperature anisotropies

After neglecting contributions from polarization and anisotropic stress

$$\left(\frac{\Delta T(\hat{n})}{T_0}\right)^{(S)}_{LSS} = \int \frac{d^3q}{(2\pi)^3}\alpha(\vec{q})e^{i\vec{q}\cdot\hat{n}r_L}$$

$$\times\left[\frac{1}{4}\Delta^{(S)}_{T,0}(q,t_L) - \frac{1}{2}a^2(t_L)\ddot{B}_q(t_L) - \frac{1}{2}a(t_L)\dot{a}(t_L)\dot{B}_q(t_L)\right.$$

$$\left. + i\mu q\left(\delta u_q(t_L)/a(t_L) + a(t_L)\dot{B}_q(t_L)/2\right)\right]$$

More on temperature anisotropies

It is interesting to compute the multipole coefficients

$$a^{(S)}_{T,\ell\, m} = 4\pi i^{\ell} \int \frac{d^3q}{(2\pi)^3} \alpha(\vec{q}) Y^*_{\ell\, m}(\hat{q})$$

$$\times \Bigg[\left(\frac{1}{4} \Delta^{(S)}_{T,0}(q,t_L) - \frac{1}{2} a^2(t_L) \ddot{B}_q(t_L) - \frac{1}{2} a(t_L) \dot{a}(t_L) \dot{B}_q(t_L) \right) \right) j_\ell(qr_L)$$

$$+ iq \left(\delta u_q(t_L)/a(t_L) + a(t_L) \dot{B}_q(t_L)/2 \right) j'_\ell(qr_L) \Bigg]$$

The behavior of the spherical Bessel functions for $\ell \gg 1$ implies that the dominant contributions arises from wave numbers

$$qr_L \approx \ell$$

More on temperature anisotropies

For the adiabatic solution modes are frozen outside the horizon. So the behavior of modes will be very different for

$$\frac{q}{a_L H_L} < 1 \quad \text{or} \quad \frac{q}{a_L H_L} > 1$$

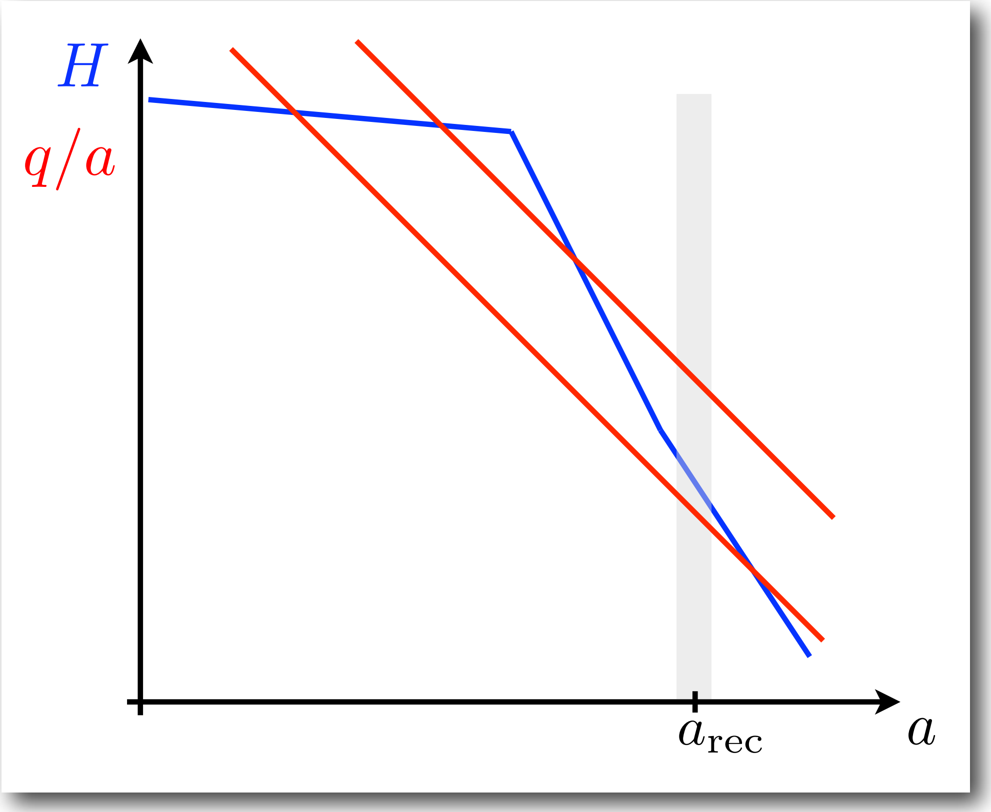

More on temperature anisotropies

Where does the transition happen?

$$\frac{q}{a_L H_L} = \frac{\ell}{a_L r_L H_L} \approx \frac{\ell}{60}$$

$\ell < 60$ contribution predominantly from modes still frozen during recombination

$\ell > 60$ contribution predominantly from modes inside the horizon during recombination

More on temperature anisotropies

For the frozen long modes we can write the multipole coefficients in terms of the curvature perturbation

$$a_{T,\ell\, m}^{(S)} \approx 4\pi i^{\ell} \int \frac{d^3 q}{(2\pi)^3} \mathcal{R}(\vec{q}) Y_{\ell\, m}^{*}(\hat{q}) \left[-\frac{1}{5} j_{\ell}(q r_L) \right]$$

and for a scale-invariant* primordial power spectrum

$$\frac{\ell(\ell+1)C_{\ell}}{2\pi} = \frac{T_0^2}{25} \Delta_{\mathcal{R}}^2$$

This is sometimes referred to as the Sachs-Wolfe plateau

(*) it can also be evaluated for the LCDM power law spectrum

More on temperature anisotropies

The short modes enter the horizon before recombination. For simplicity we will consider modes that enter during radiation domination.

$$\frac{q}{a_{eq}H_{eq}} = \frac{\ell}{a_{eq}r_L H_{eq}} \approx \frac{\ell}{140} \gg 1$$

When the modes enter a large number of free electrons are present and we can expand in $q/a\omega_c$.

This is referred to as the tight-coupling expansion.

More on temperature anisotropies

At leading order, the Boltzmann hierarchy reduces to the hydrodynamics, and the solutions are sound waves.
The Sachs-Wolfe contribution takes the form

$$a^{(S)}_{T,\ell\, m} = 4\pi i^{\ell} \int \frac{d^3q}{(2\pi)^3} \mathcal{R}(\vec{q}) Y^*_{\ell\, m}(\hat{q})$$

$$\times \left[\frac{3}{5} \mathcal{T}(q) R_L - \frac{1}{(1+R_L)^{1/4}} \cos(q r_s) \right] j_\ell(q r_L)$$

with

$$R = \frac{3}{4} \frac{\rho_b}{\rho_\gamma}$$ baryon loading

$$r_s = \int_0^{t_L} \frac{dt}{a(t)\sqrt{3(1+R(t))}}$$ (comoving) sound horizon

$$\mathcal{T}(q)$$ transfer function

More on temperature anisotropies

There are two effects we have ignored in this approximation.

1. The solutions oscillate around last scattering and the finite width of the last scattering surface leads to damping.

2. The mean free path of the photons becomes comparable to the momentum of the modes for large q which leads to Silk damping.

$$a^{(S)}_{T,\ell\, m} = 4\pi i^{\ell} \int \frac{d^3q}{(2\pi)^3} \mathcal{R}(\vec{q}) Y^*_{\ell\, m}(\hat{q})$$

$$\times \left[\frac{3}{5} \mathcal{T}(q) R_L - \frac{e^{-\int_0^{t_L} \Gamma(q,t) dt}}{(1+R_L)^{1/4}} \cos(qr_s) \right] j_\ell(qr_L)$$

More on temperature anisotropies

Including the Doppler contribution

$$a^{(S)}_{T,\ell\, m} = 4\pi i^\ell \int \frac{d^3q}{(2\pi)^3}\mathcal{R}(\vec{q})Y^*_{\ell\, m}(\hat{q})$$

$$\times\left\{\left[\frac{3}{5}\mathcal{T}(q)R_L - \frac{e^{-\int_0^{t_L}\Gamma(q,t)dt}}{(1+R_L)^{1/4}}\cos(qr_s)\right]j_\ell(qr_L)\right.$$

$$\left. - \left[\frac{\sqrt{3}e^{-\int_0^{t_L}\Gamma(q,t)dt}}{(1+R_L)^{3/4}}\sin(qr_s)\right]j'_\ell(qr_L)\right\}$$

- Since the integral is dominated by $q \approx \ell/r_L$, the peak positions are set by $\theta = r_s/r_L$, which e.g. probes curvature.

- Since $R \propto \Omega_b$ the relative height of the peaks is a sensitive probe of the baryon abundance.

- The damping scale probes the mean free path of the photons and thus, for example, the Helium abundance.

More on temperature anisotropies

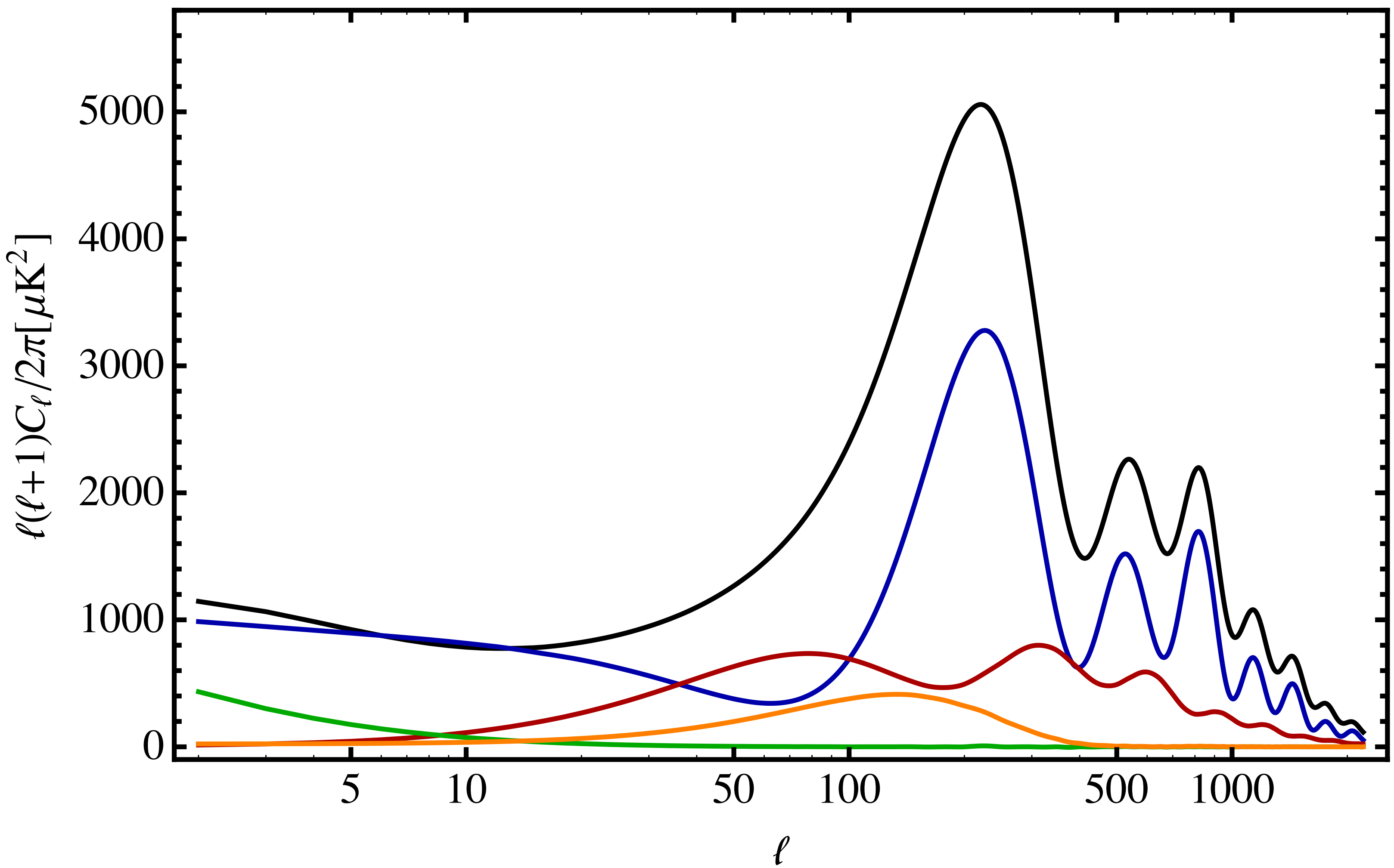

B-mode search

In addition to the density perturbations, inflation also predicts a nearly scale invariant spectrum of gravitational waves

$$\dot{\tilde{\Delta}}^{(T)}_{T,\ell}(q,t) + \frac{q}{a(2\ell+1)}\left[(\ell+1)\tilde{\Delta}^{(T)}_{T,\ell+1}(q,t) - \ell\tilde{\Delta}^{(T)}_{T,\ell-1}(q,t)\right]$$

$$= \left(-2\dot{\mathcal{D}}_q(t) + \omega_c(t)\Psi(q,t)\right)\,\delta_{\ell,0} - \omega_c(t)\tilde{\Delta}^{(T)}_{T,\ell}(q,t)$$

$$\dot{\tilde{\Delta}}^{(T)}_{P,\ell}(q,t) + \frac{q}{a(2\ell+1)}\left[(\ell+1)\tilde{\Delta}^{(T)}_{P,\ell+1}(q,t) - \ell\tilde{\Delta}^{(T)}_{P,\ell-1}(q,t)\right]$$

$$= -\omega_c(t)\Psi(q,t)\,\delta_{\ell,0} - \omega_c(t)\tilde{\Delta}^{(T)}_{P,\ell}(q,t)$$

with

$$\Psi(q,t) = \frac{1}{10}\tilde{\Delta}^{(T)}_{T,0}(q,t) + \frac{1}{7}\tilde{\Delta}^{(T)}_{T,2}(q,t) + \frac{3}{70}\tilde{\Delta}^{(T)}_{T,4}(q,t)$$
$$-\frac{3}{5}\tilde{\Delta}^{(T)}_{P,0}(q,t) + \frac{6}{7}\tilde{\Delta}^{(T)}_{P,2}(q,t) - \frac{3}{70}\tilde{\Delta}^{(T)}_{P,4}(q,t)$$

B-mode search

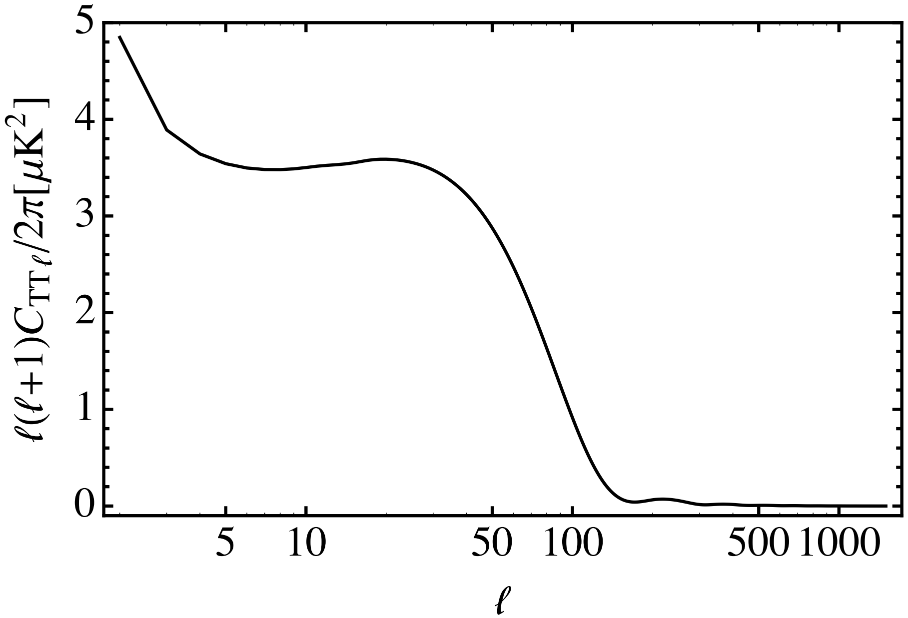

In addition to TT, TE, EE, primordial gravitational waves generate BB

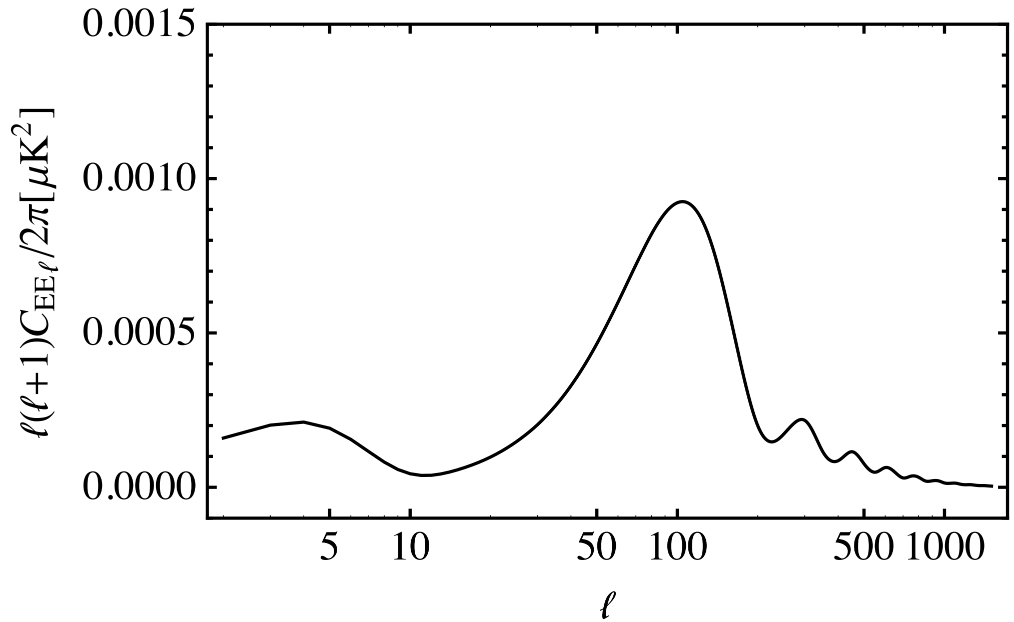

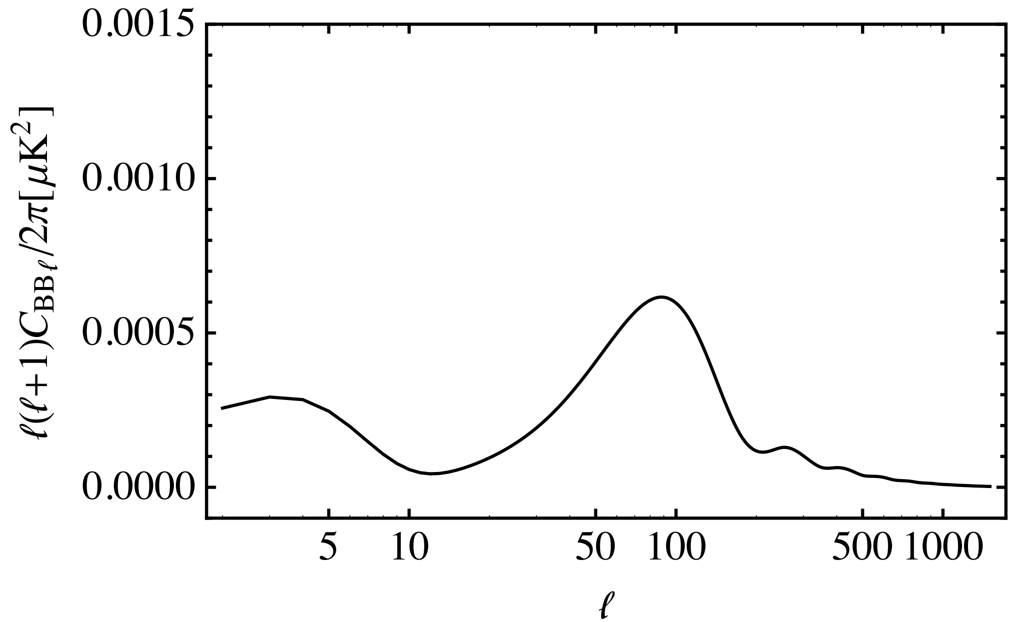

B-mode search

The power spectrum of primordial gravitational waves generated by inflation is

$$\Delta_h^2(k) = \frac{2H^2(t_k)}{\pi^2}$$

A measurement of the tensor contribution would provide a direct measurement of the expansion rate of the universe during inflation, as well as the energy scale

$$V_{\rm inf}^{1/4} = 1.06 \times 10^{16}\, GeV \left(\frac{r}{0.01}\right)^{1/4}$$

with $\quad r = \frac{\Delta_h^2}{\Delta_{\mathcal{R}}^2}$

B-mode search

- For r>0.01 the inflaton must have moved over a super-Planckian distance in field space.
- Motion of the scalar field over super-Planckian distances is hard to control in an effective field theory

$$V(\phi) = V_0 + \frac{1}{2}m^2\phi^2 + \frac{1}{3}\mu\phi^3 + \frac{1}{4}\lambda\phi^4 + \phi^4 \sum_{n=1}^{\infty} c_n \left(\phi/\Lambda\right)^n$$

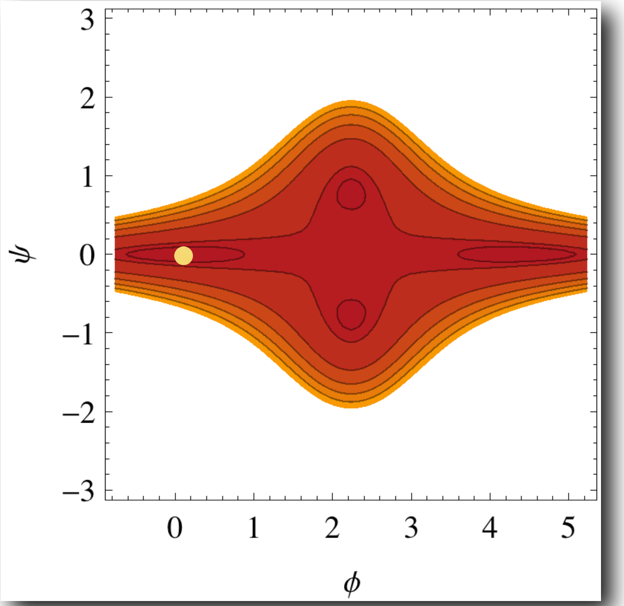

B-mode search

Possible Solution:

Use a field with a shift symmetry and break the shift symmetry in a controlled way.

e.g. Linde's chaotic inflation with

$$V(\phi) = \frac{1}{2} m^2 \phi^2 \qquad \text{with} \qquad m \ll M_p$$

In field theory we may simply postulate such a symmetry, but it is far from obvious that such shift symmetries exist in a theory of quantum gravity.

So a detection of primordial gravitational waves might teach us about shift symmetries in quantum gravity.

B-mode search

BICEP2 polarization data

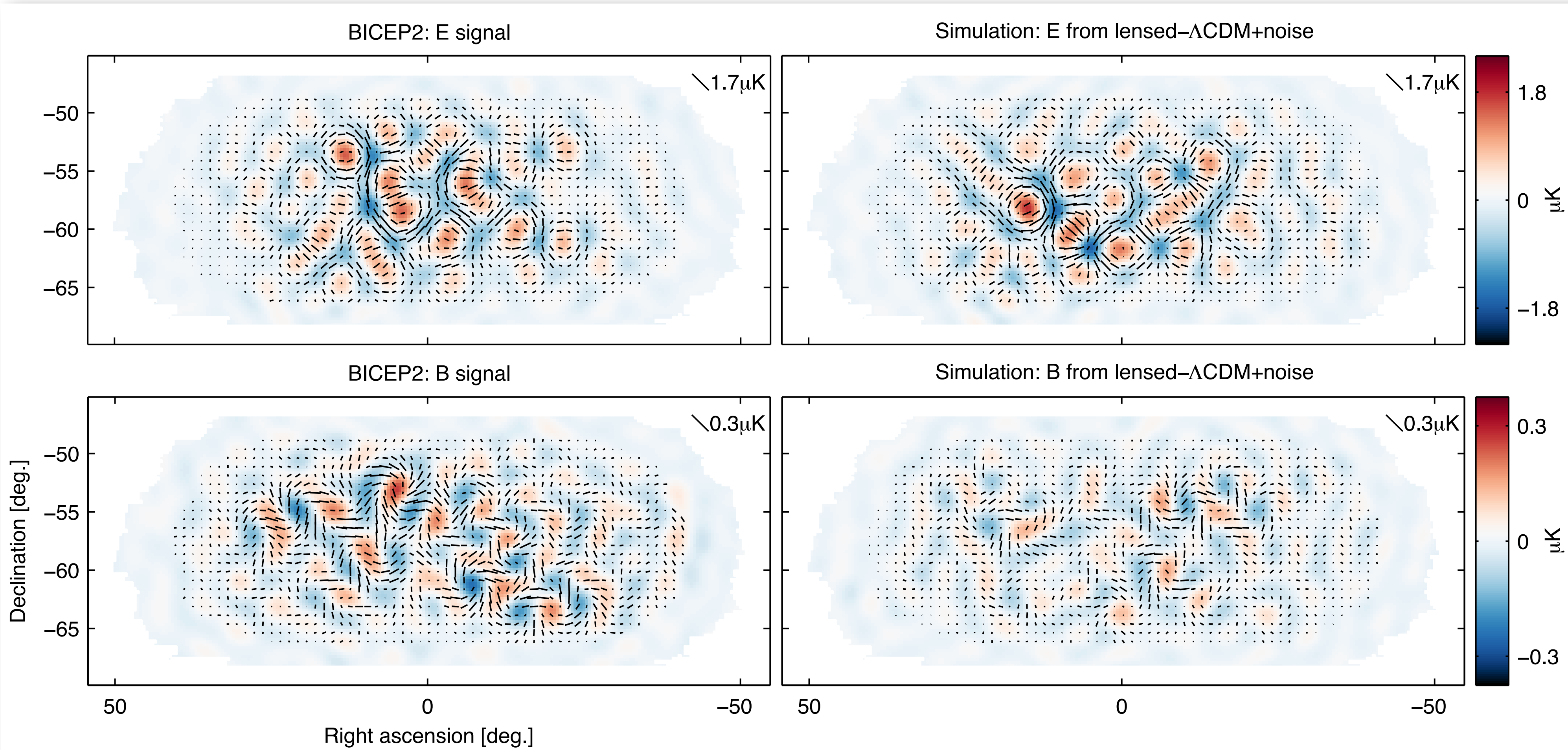

Noise level: 87 nK deg - the deepest map at 150 GHz of this patch of sky

(Planck noise level: few μK deg)

B-mode search

Foreground models made in collaboration with David Spergel, Colin Hill, and Aurelien Fraisse

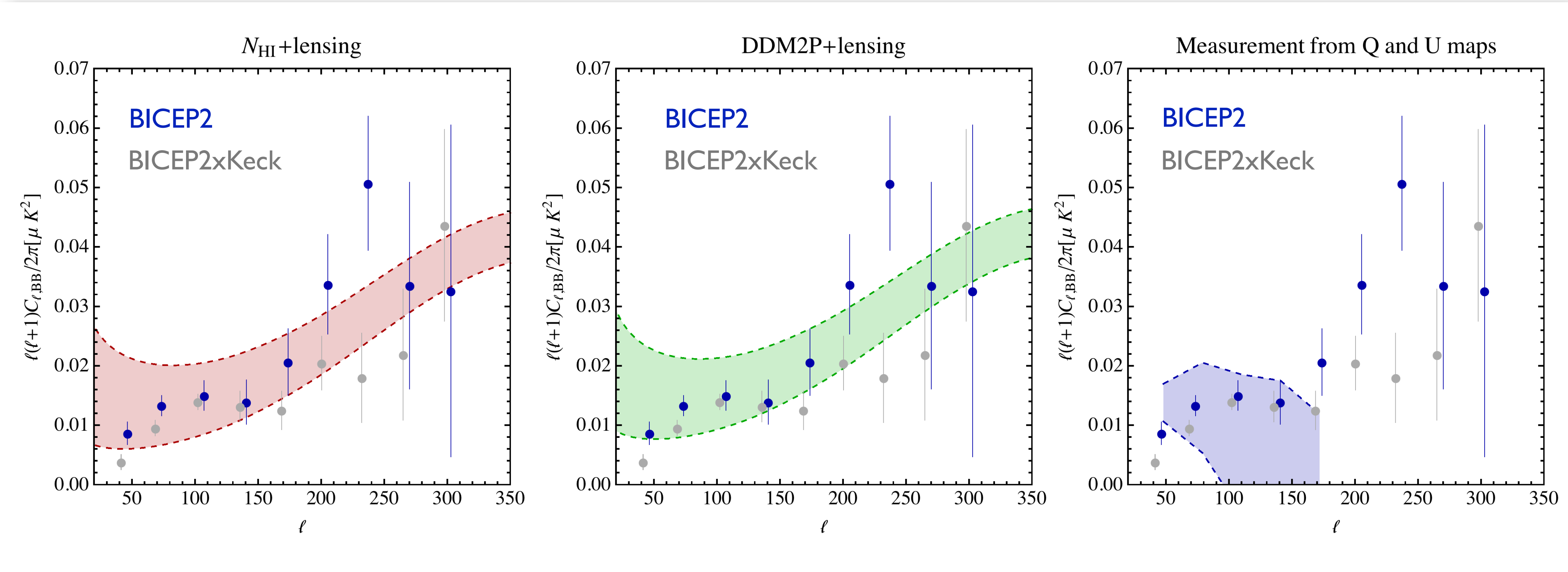

B-mode search

- measurement of BB in the BICEP2 region at 353 GHz rescaled to 150 GHz

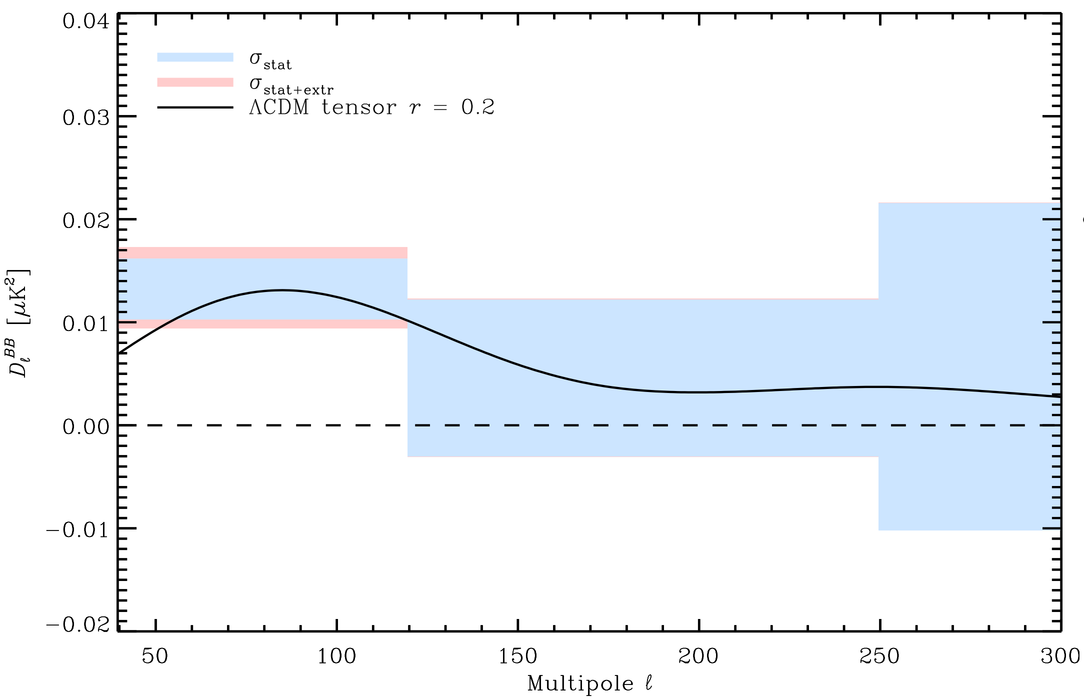

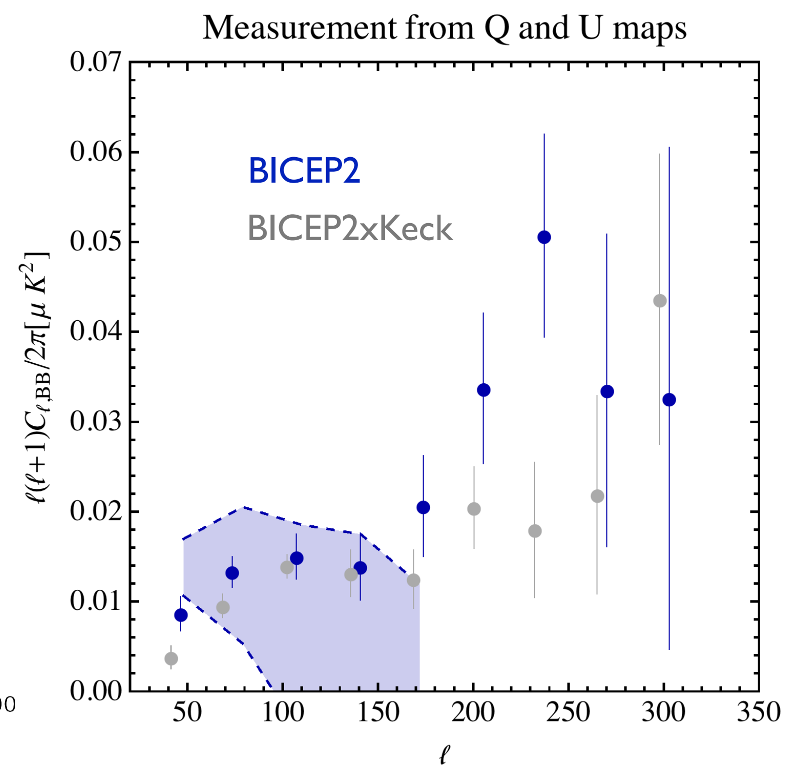

$$D_\ell^{BB} = 1.32 \times 10^{-2}\, \mu\mathrm{K}^2_{\mathrm{CMB}}$$

B-mode search

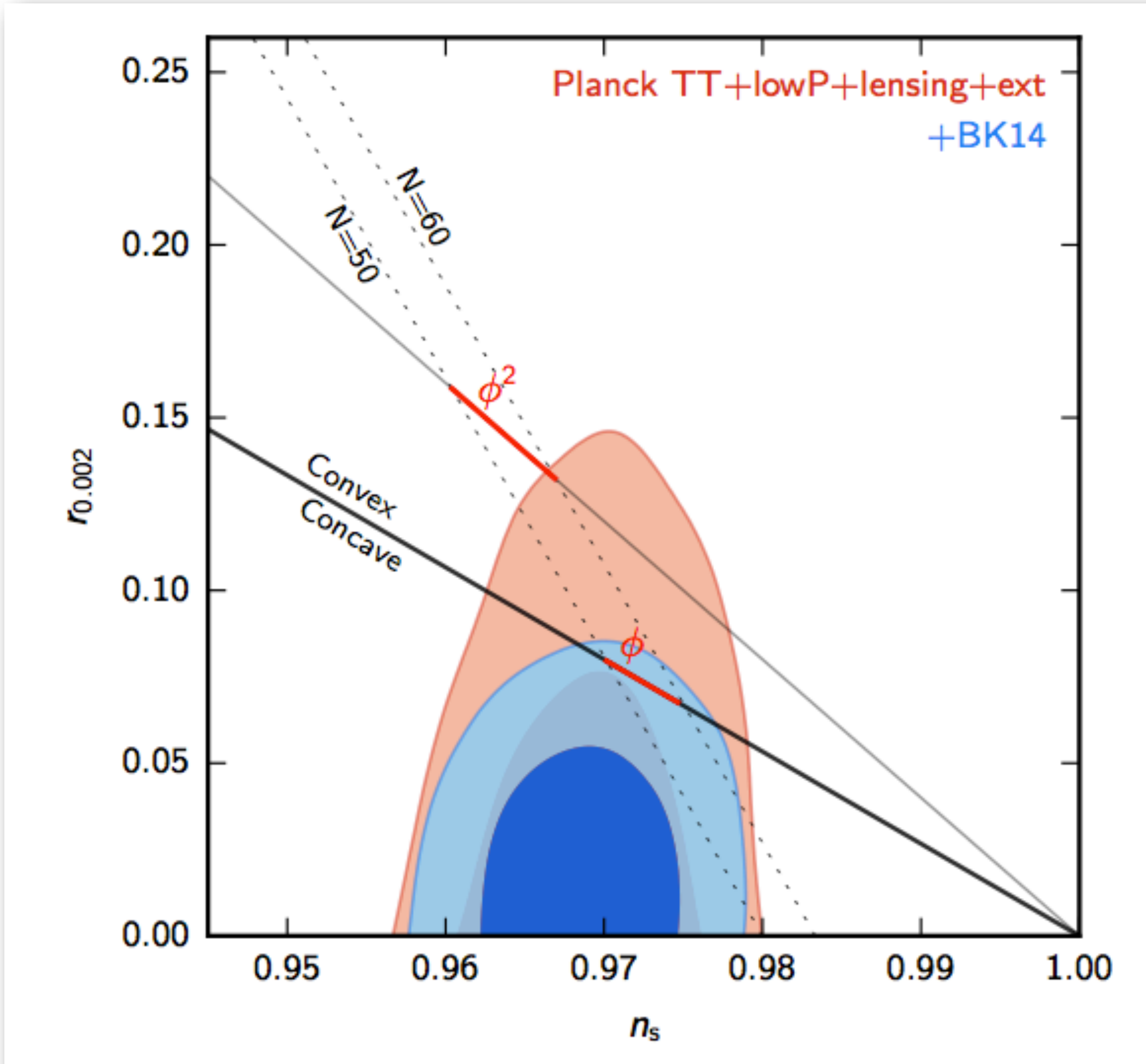

B-mode search

With the current data, we can constrain r by

- the tensor contribution to the temperature anisotropies on large angular scales
- the B-mode polarization generated by tensors.

The two likelihood are essentially independent

$$\mathcal{L}(r_{TT}, r_{BB}) = \mathcal{L}_{TT}(r_{TT})\mathcal{L}_{BB}(r_{BB})$$

Typically we talk about $\mathcal{L}(r, r)$

B-mode search

$\mathcal{L}(r_{TT}, r_{BB})$ before BICEP2

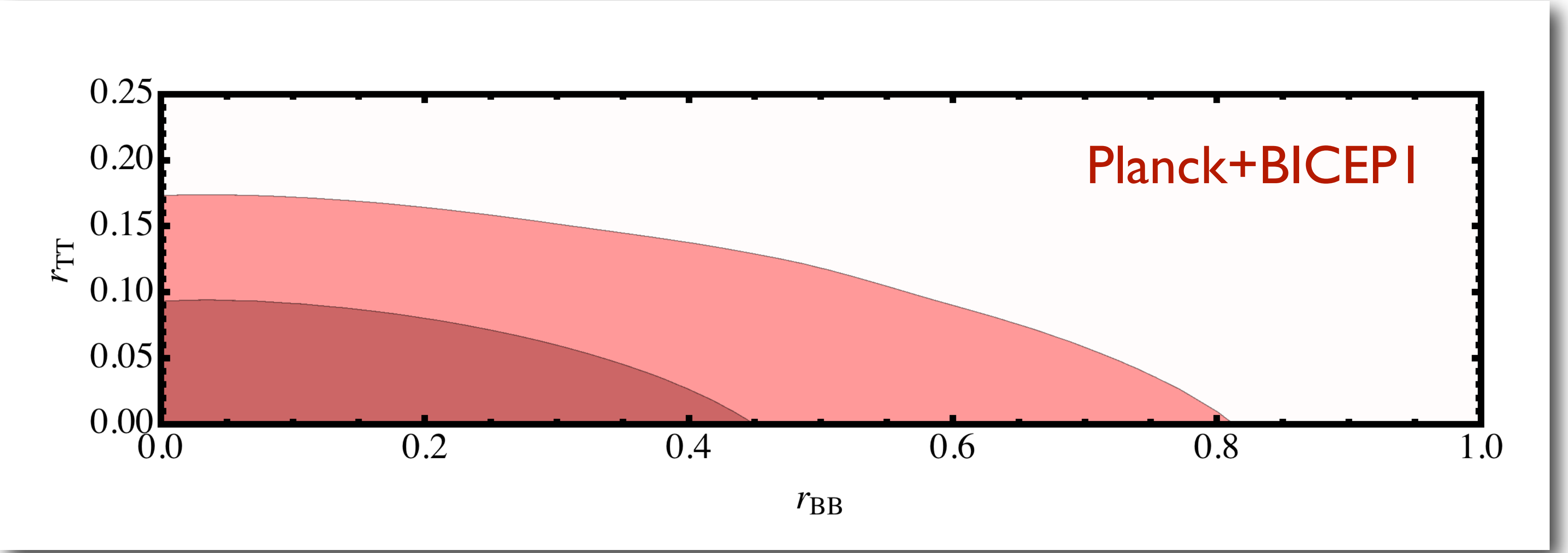

Constraint dominated by temperature data

B-mode search

$\mathcal{L}(r_{TT}, r_{BB})$ after BICEP2

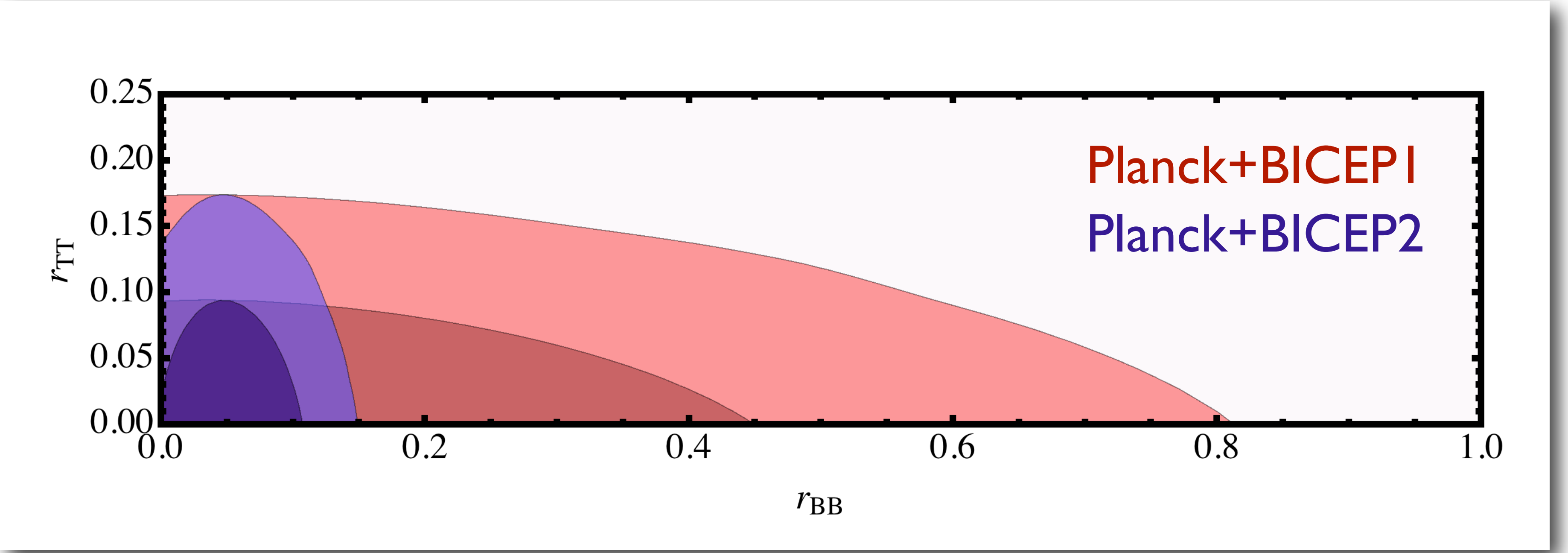

Constraint from polarization data comparable to constraint from temperature and will soon be significantly stronger.

B-mode search

$\mathcal{L}(r_{TT}, r_{BB})$ after BK14

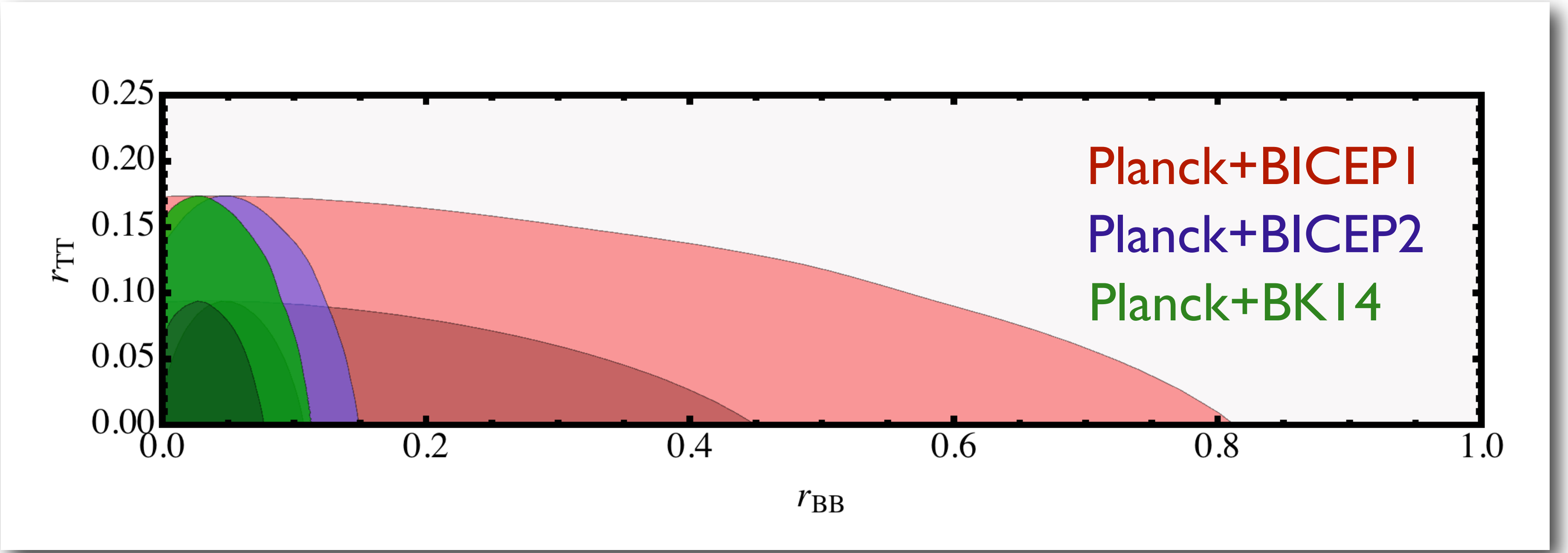

Constraint from polarization data comparable to constraint from temperature and will soon be significantly stronger.

Outlook

ongoing and upcoming:

Ground: BICEP2, Keck Array, BICEP3, SPTPol/SPT3G, ACTPol/AdvACT, ABS, CLASS, POLARBEAR/Simons Array, C-BASS, QUIJOTE, B-Machine, Simons Observatory

Balloon: EBEX, SPIDER, PIPER

future (>5 years)

Ground: CMB Stage IV

Satellite: LiteBIRD, PIXIE,...

Outlook

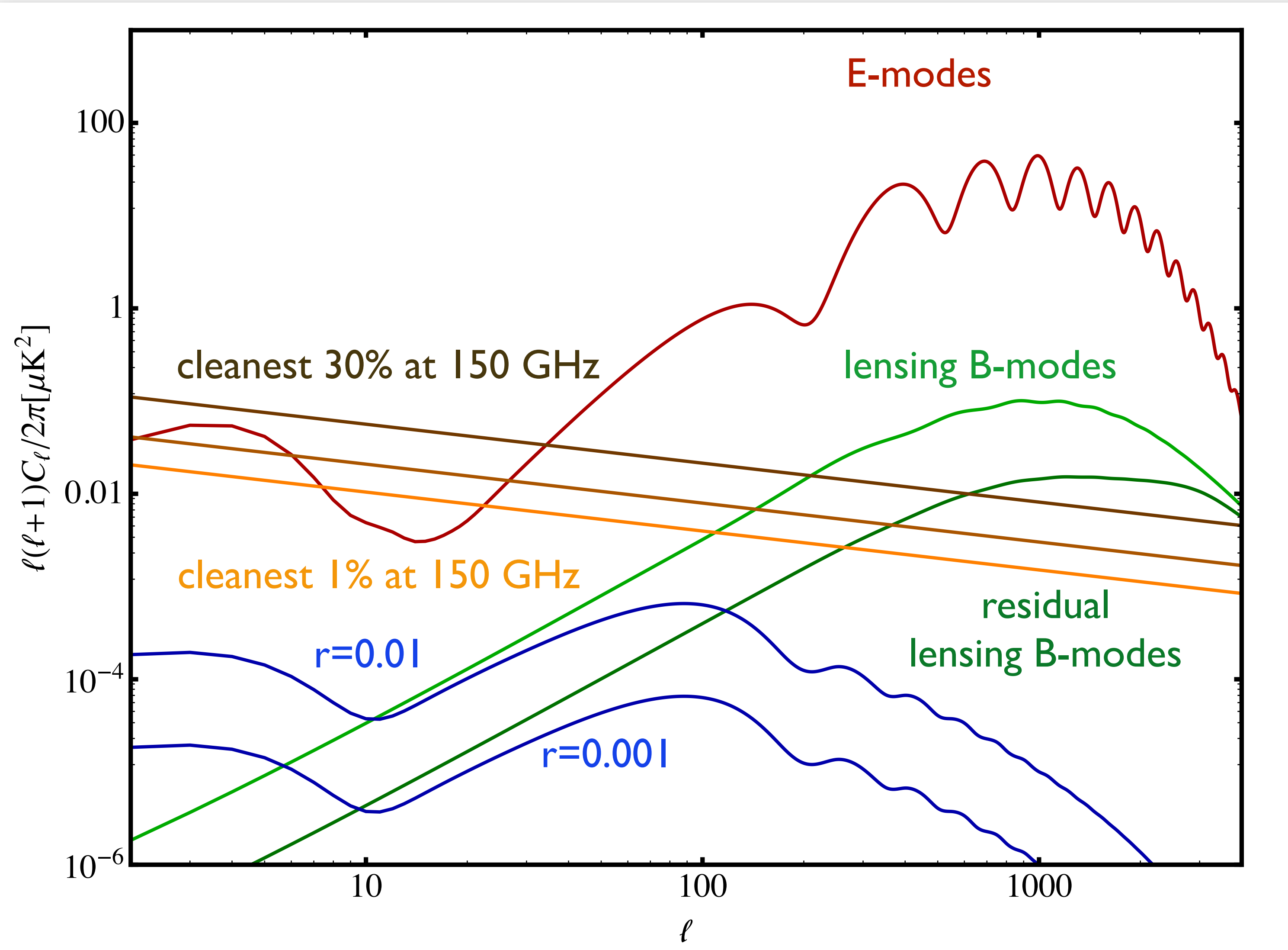
E-modes
lensing B-modes
cleanest 30% at 150 GHz
cleanest 1% at 150 GHz
residual
lensing B-modes
r=0.01
r=0.001
100
1
0.01
10^{-4}
10^{-6}
10
100
1000
ℓ
$\ell(\ell+1)C_\ell/2\pi[\mu K^2]$

Outlook

Forecasting exactly how well it can do is difficult given our current level of understanding of foregrounds.

Models for polarized foreground need three ingredients, typically

- Intensity map
- Polarization fraction
- Polarization angles

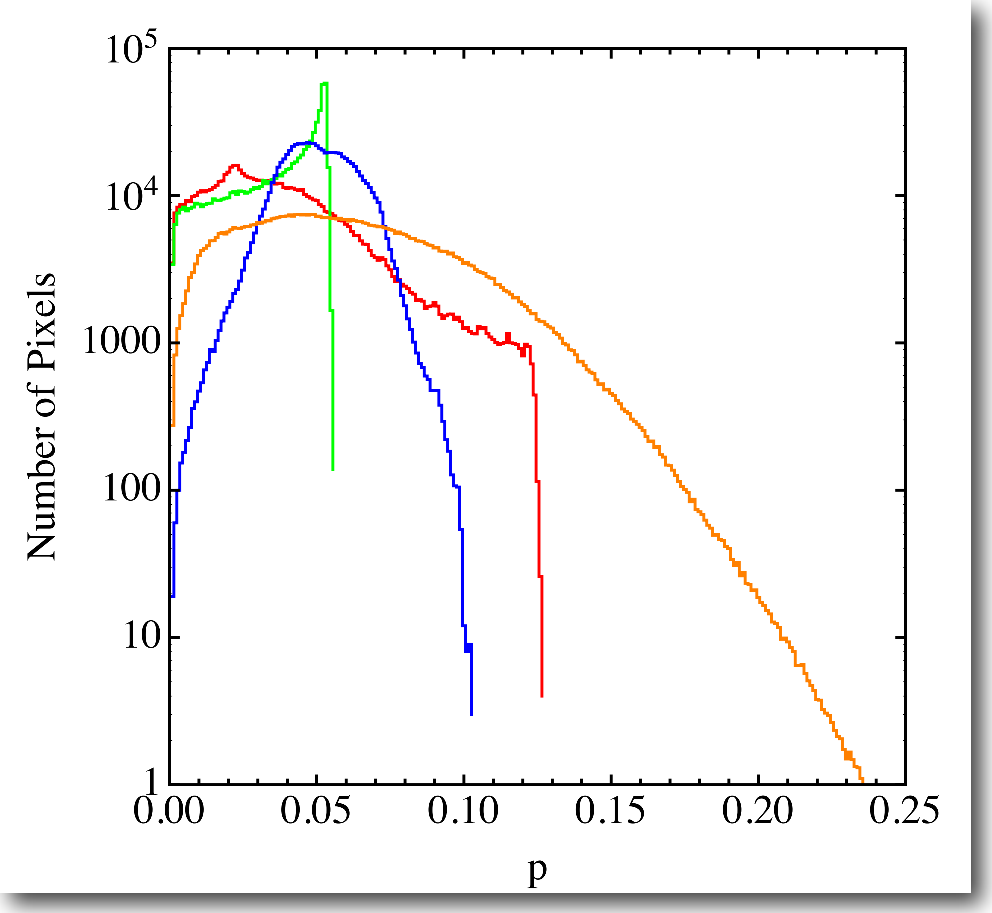

Planck helps on large scales at frequencies 150 GHz and up.

Outlook

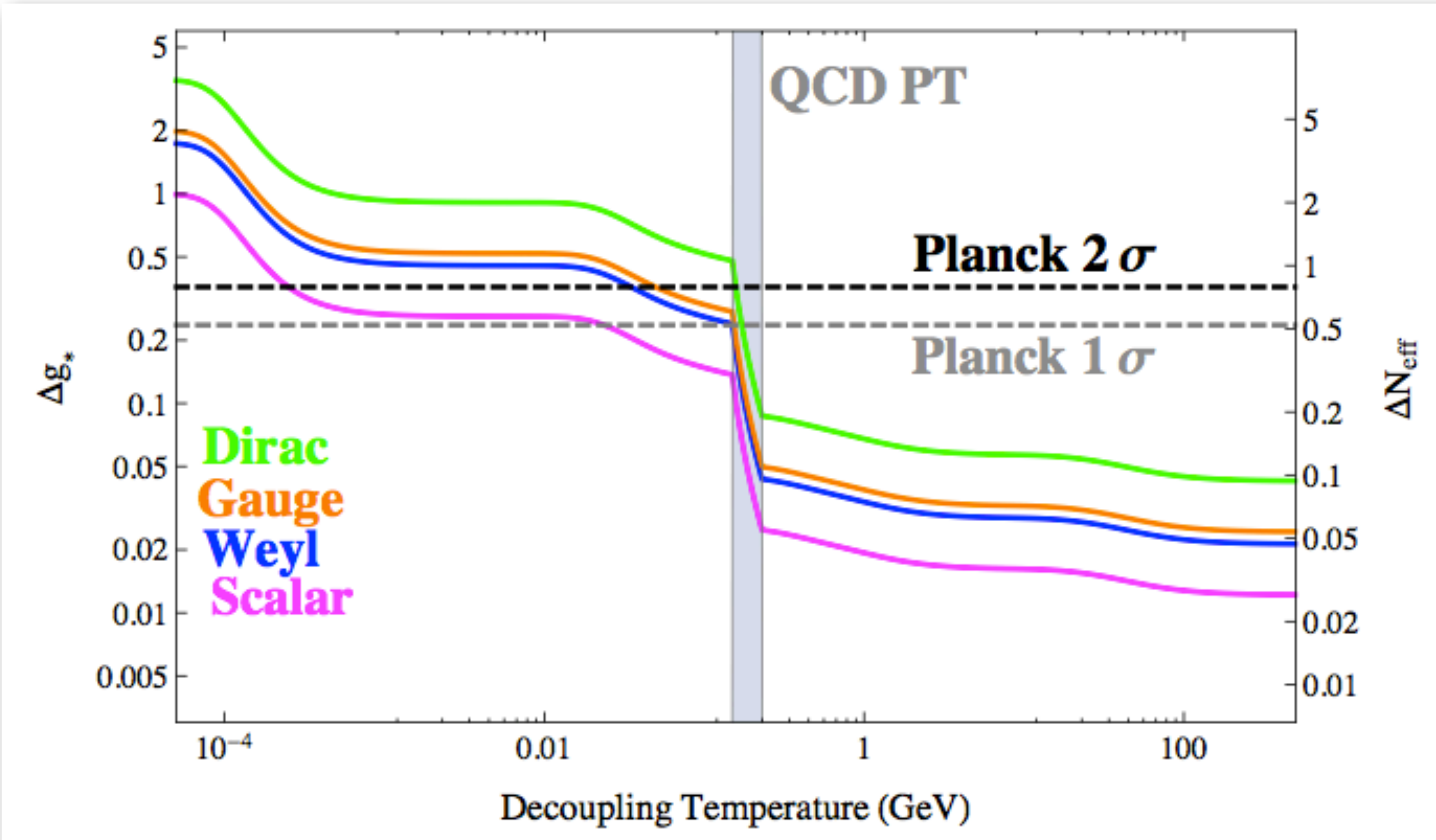

$$\sigma_{\rm CMBS4}(N_{\rm eff}) \approx 0.02$$

(Brust, Kaplan, Walters 1303.5079)

Conclusions

- I hope you know slightly more about the CMB than you did before
- The CMB has provided us with valuable information about the early universe for 51 years and will continue to do so.
- We may detect primordial gravitational waves, measure neutrino masses, the number of effective relativistic degrees of freedom, dark matter, ...
- Large scale structure surveys will provide a useful counter part
- The next decade should be very interesting in cosmology

Thank you